IOP Publishing Phys. Med. Biol. 65 (2020) 085016 https://doi.org/10.1088/1361-6560/ab7b30

Physics in Medicine & Biology

IPEM Institute of Physics and Engineering in Medicine

RECEIVED
8 November 2019

REVISED
24 February 2020

ACCEPTED FOR PUBLICATION
28 February 2020

PUBLISHED
23 April 2020

PAPER

The influence of lack of reference conditions on dosimetry in pre-clinical radiotherapy with medium energy x-ray beams

Anna Subiel[1,8], Ileana Silvestre Patallo[1], Hugo Palmans[1,2], Miriam Barry[1], Amanda Tulk[3], Georgios Soultanidis[4], John Greenman[5], Victoria L Green[5], Christopher Cawthorne[6] and Giuseppe Schettino[1,7]

[1] National Physical Laboratory, Hampton Road, Teddington, Middlesex TW11 0LW, United Kingdom
[2] MedAustron, Marie-Curiestrasse 5, A-2700, Wiener Neustadt, Austria
[3] Xstrahl Ltd, Riverside Way, Camberley, Surrey GU15 3YL, United Kingdom
[4] Biomedical Engineering and Imaging Institute, Icahn School of Medicine at Mount Sinai, New York, United States of America
[5] University of Hull, Cottingham Road, East Riding of Yorkshire, Hull HU6 7RX, United Kingdom
[6] Molecular Small Animal Imaging Centre (MoSAIC), KU Leuven, Leuven, Belgium
[7] University of Surrey, Guilford, United Kingdom
[8] Author to whom any correspondence should be addressed.

E-mail: anna.subiel@npl.co.uk

Keywords: backscatter, pre-clinical dosimetry, medium energy x-rays, lack of reference conditions, radiobiology

Abstract

Despite well-established dosimetry in clinical radiotherapy, dose measurements in pre-clinical and radiobiology studies are frequently inadequate, thus undermining the reliability and reproducibility of published findings. The lack of suitable dosimetry protocols, coupled with the increasing complexity of pre-clinical irradiation platforms, undermines confidence in preclinical studies and represents a serious obstacle in the translation to clinical practice. To accurately measure output of a pre-clinical radiotherapy unit, appropriate Codes of Practice (CoP) for medium energy x-rays needs to be employed. However, determination of absorbed dose to water (D_w) relies on application of backscatter factor (B_w) employing in-air method or carrying out in-phantom measurement at the reference depth of 2 cm in a full backscatter (i.e. $30 \times 30 \times 30$ cm^3) condition. Both of these methods require thickness of at least 30 cm of underlying material, which are never fulfilled in typical pre-clinical irradiations. This work is focused on evaluation the effects of the lack of recommended reference conditions in dosimetry measurements for pre-clinical settings and is aimed at extending the recommendations of the current CoP to practical experimental conditions and highlighting the potential impact of the lack of correct backscatter considerations on radiobiological studies.

1. Introduction

Orthovoltage x-ray beams in the range of 0.5–4 mm Cu half-value layer (HVL) are widely used in pre-clinical radiation research both for *in vivo* and *in vitro* irradiations. Their relatively easy shielding properties result in small cabinets which can be housed in conventional laboratories and allow partial sample irradiation without sophisticated equipment. Their attenuation in water is adequate to provide uniform dose distributions in shallow samples and the resulting biological damage is very similar to that produced by ^{60}Co reference radiation. Dose-response relationships, however, are often very steep, with small changes in the absorbed dose resulting in large variations in observed radiobiological response. According to ICRU Report 24, a change of 7%–10% in absorbed dose to the target volume results in a significant change in tumour control probability (TCP) (Brahme 1984). Despite well-established dosimetry methodologies and procedures in clinical radiotherapy, dose measurements in pre-clinical and radiobiology studies are frequently inadequate, thus undermining the reliability and reproducibility of the published findings. An expanded uncertainty of 5% ($k = 2$) in the delivery of absorbed dose has been agreed for clinical studies and such constraints should also be applied to pre-clinical investigations (ICRU 1976). Even the 1985 European Late Effects Project Group (EULAP) report (Zoetelief *et al* 1985), describing the results of x-ray dosimetry comparisons in Europe failed

to follow the constraints of combined uncertainty of 5%, which has been revised in the follow-up protocol published in 2001 (Zoetelief *et al* 2001). The lack of suitable dosimetry protocols, coupled with the increasing complexity of pre-clinical irradiation platforms (Verhaegen *et al* 2018), represents a serious obstacle in the translation of radiobiological research into clinical practice (Nature 2018). These concerns have already been emphasized in a report by Desrosiers *et al* (2013) where a list of highlighted issues and recommendations have been published. More recently Draeger *et al* (2020) published comprehensive review demonstrating a deep lack of reporting basic physics concepts in pre-clinical radiation research literature.

It is of crucial importance that accurate and traceable radiation doses are delivered to each of the samples in pre-clinical radiation studies. In addition, for these experiments to be adequately interpreted, compared and reproduced, a detailed description of the dosimetry parameters should be included in any radiobiology publication (Desrosiers *et al* 2013). In *in vitro* irradiations, typically an absorbed dose on or near the surface of the irradiated sample is the quantity that needs to be determined as accurately as possible (Kim *et al* 2010). However, the existing protocols (Klevenhagen *et al* 1996, Ma *et al* 2001, Aukett *et al* 2005) provide guidance on dosimetric characterization for clinically relevant and established reference conditions. The constraints of pre-clinical x-ray cabinets and the wide range of samples and devices employed in radiobiological studies result in experimental setups which, from a dosimetric point of view, differ significantly from reference conditions and present dosimetry challenges which need to be addressed on individual basis.

It has been reported that about half of all preclinical research in the United States is not reproducible (Guterman 2015). The inadequacy of dosimetry reporting in published radiobiology studies is one of the main issues and it both adds to concerns that the dosimetry is not being adequately performed and it limits reproducibility of the research. Ultimately, this brings the published experimental results and conclusions into question. Yoshizumi *et al* asserted that experiments performed without accurate and reproducible dosimetry were wasted (Yoshizumi *et al* 2011) and potentially hampered the translation of new clinical approaches. Lu *et al* (2013) stated that planned dose was commonly derived by multiplying dose rate, derived from air kerma measured in absence of the setup, with time. The dose rate in the actual setup, however, is considerably different due to different attenuation and scatter conditions between the experimental setup used for dose output measurement and the actual sample exposure. The scatter dose plays a significant role particularly for soft x-ray beams where non-negligible differences can be introduced by small changes in the experimental setup.

The available data reporting on the change in backscatter with the thickness of underlying material has been published by Klevenhagen (1982) in 1982. Using a purposely build device, the author experimentally investigated the influence of the thickness of underlying material on the magnitude of BSF for radiation beam qualities (1 mm Al to 8 mm Al) much lower than commonly used in pre-clinical irradiators. More recently, Chen *et al* (2019) demonstrated the magnitude of dose error, reaching 50% dose difference for the specific beam parameters that results from insufficient backscatter in commercial pre-clinical irradiation systems, such as XRAD-225 (Precision x-ray Inc.) or SARRP (Xstrahl Inc.). The authors provided a comprehensive set of lookup tables with backscatter factors as a function of phantom thickness to account for this issue for four specific beam qualities that can be generated by these commercial systems for square fields up to 20 cm. Moreover, the depth dose curves for the studied four cases were generated for the selected beam qualities. In this study, we extend Klevenhagen's investigations (Klevenhagen 1982) to a wide range of medium energy x-ray beams using experimentally validated Monte Carlo (MC) simulations with EGSnrc (Kawrakow *et al* 2018) to generate reference data sets. The purpose of this work was three-fold: (i) to formulate a set of analytical expressions to allow for the determination of the correction factors associated with lack of full backscatter conditions for a wide range of HVLs between 0.5 and 4 mm Cu and field sizes ranging from 1 to 30 cm diameter when using the in-air method, (ii) to assess the thickness of underlying water thickness required to fulfil the full backscatter conditions for in-phantom formalism and (iii) to investigate the change of the relative depth dose distributions with decreasing thickness of underlying material. In contrast to Chen's work, where purpose (ii) and (iii) were also addressed for the selected HVLs, this study provides generic expressions allowing calculation of the factor enabling correction for lack of full backscatter conditions for any beam quality between 0.5 and 4 mm Cu HVL. It also provides an independent validation of the backscatter values estimated by Chen *et al* (2019) This study aims to allow users of orthovoltage x-ray irradiators to retrieve the required correction factor to compensate for lack of reference irradiation condition in pre-clinical set-ups using the available CoPs.

2. Methodology

2.1. Dosimetry formalism for medium energy x-ray beams

To measure output of a pre-clinical radiotherapy unit accurately, appropriate Codes of Practice (CoP) (Klevenhagen *et al* 1996, Ma *et al* 2001, Aukett *et al* 2005) for the dosimetry of medium energy x-rays using

calibrated ionization chambers need to be employed. Two approaches can be followed: in-air and in-phantom methods.

For the in-air method, the absorbed dose should be determined by taking in-air measurements and applying a backscatter factor (BSF) to account for the setup in which the samples are placed (Klevenhagen *et al* 1996, Ma *et al* 2001, Aukett *et al* 2005, Mayles *et al* 2007). The BSF is defined as the ratio between a dose quantity measured (or calculated) on the central axis at the surface of a phantom facing the radiation source and the dose quantity at the same position free in air (Mayles *et al* 2007). In this method, the absorbed dose is determined by positioning the ionization chamber, free-in-air, to measure air kerma (K_{air}). From this quantity, the absorbed dose at the surface of a water phantom is derived by using two factors: the mass-energy absorption coefficient of water to air in air and the BSF. The following equation is used to determine the absorbed dose to water at the surface of a water phantom $D_{w,z=0}$:

$$D_{w,z=0} = MN_K B_w \left[\left(\frac{\bar{\mu}_{en}}{\rho} \right)_{air}^{water} \right]_{air}, \tag{1}$$

where M is the reading of the ionization chamber converted to standard conditions for temperature and pressure, N_K is the air-kerma calibration coefficient of the ionization chamber for the particular HVL of the radiation beam, B_w is the BSF in water for the particular field size and beam quality and $\left[\left(\frac{\bar{\mu}_{en}}{\rho} \right)_{air}^{water} \right]_{air}$ is the mass–energy absorption coefficient ratio of water to air for the primary x-ray spectrum. The B_w values are given in beam data tables (for example in Ma *et al* 2001), as a function of field size (ϕ) and beam quality (HVL). This calibration method can be used over a wide energy range from 40 to 300 kVp (Klevenhagen *et al* 1996, Ma *et al* 2001, Aukett *et al* 2005) and it is particularly indicated for assessment of absorbed dose in volumes in close proximity of the sample surface.

Alternatively, the in-phantom method for reference dosimetry of kilovoltage x-ray beams requires the measurement of the dose in a water phantom at a reference depth of typically 2 cm (Klevenhagen *et al* 1996, Ma *et al* 2001). The ionization chamber is positioned at a depth of 2 cm within the water phantom and the dose, $D_{w,z=2}$, at this point is determined by:

$$D_{w,z=2} = MN_K k_{ch} \left[\left(\frac{\bar{\mu}_{en}}{\rho} \right)_{air}^{water} \right]_{z=2,\phi}, \tag{2}$$

where M is the reading of the ionization chamber corrected for ion recombination and the polarity effect and converted to standard conditions for temperature and pressure, N_K is the air-kerma calibration coefficient for the chamber at the particular HVL of the radiation beam, k_{ch} is a correction factor that takes into account the change in response of the ionization chamber from the calibration in air to the measurements within the water phantom and $\left[\left(\frac{\bar{\mu}_{en}}{\rho} \right)_{air}^{water} \right]_{z=2,\phi}$ is the mass-energy absorption coefficient ratio of water to air, for the x-ray spectrum in water at a depth of 2 cm for the particular diameter, ϕ, of the radiation beam. This method is recommended for x-ray beams with an HVL between 0.5 and 4 mm of Cu which, according to a dosimetry survey of pre-clinical units in the UK (InnovateUK 2018) including the vast majority of pre-clinical irradiators.

In both cases, radiation scattering plays a significant role which needs to be addressed and quantified. The determination of absorbed dose to water (D_w) relies on the use of backscatter factors (B_w) for a given source to surface distance (SSD) employing the in-air method or carrying out in-phantom measurement at the reference depth of 2 cm in a full backscatter condition (i.e. a 30 × 30 × 30 cm^3 phantom (Ma *et al* 2001) used commonly in clinics) because the mass-energy absorption coefficient ratios water to air in CoPs have been calculated for those conditions. As backscatter factors are currently only available in full backscattering conditions, both of these methods require thickness of at least 30 cm of underlying material, which are never fulfilled in typical pre-clinical irradiations. If these conditions are not met, it is essential to establish the influence of the thickness of underlying material on BSF.

2.2. Fractional backscatter in determination of $D_{w,z=0}$

The data presented in this work were generated using Monte Carlo simulations employing the DOSRZnrc user code (Rogers *et al* 2018) that forms part of the EGSnrc system (release 2018) (Kawrakow *et al* 2018). The photon and electron transport cut-off energies were both set to 10 keV, which corresponds to PCUT = 0.01 MeV and ECUT = 0.521 MeV, respectively. The low energy photon processes, i.e. bound

Table 1. Medium-energy x-ray qualities used for therapy level calibrations at NPL with inherent filtration of 0.3 mm aluminium equivalent and 4.8 mm of Perspex (Bass *et al* 2019).

		Additional filtration		
HVL [mm Cu]	Nominal generating tube potential [kV]	[mm Sn]	[mm Cu]	[mm Al]
0.5	135	—	0.27	1.2
1	180	—	0.54	1.0
2	220	—	1.40	0.9
4	280	1.5	0.26	1.0

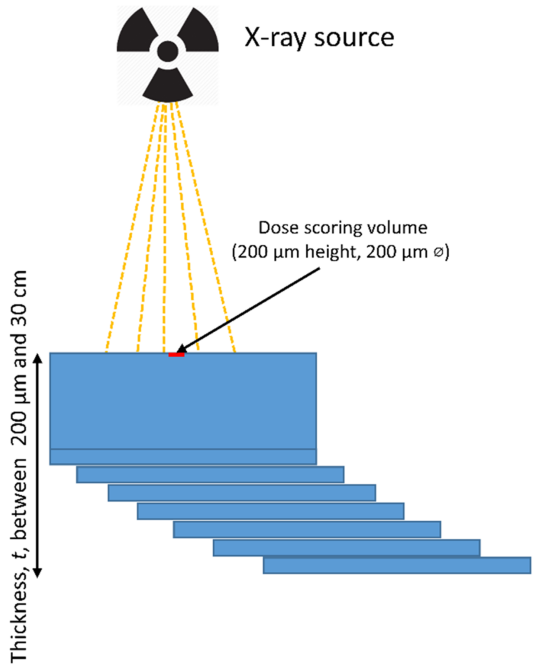

Figure 1. Setup for the calculation of backscatter build-up curves.

Compton scattering, Rayleigh scattering and atomic relaxations were included in the simulations. Photon cross-section data were taken from the XCOM database (Berger and Hubbell 1987, Hubbell and Seltzer 2004). Data sets for all materials used were generated employing the PEGS4 user code. Electron range rejection was used with the ESAVEIN parameter set to 1. The x-ray source was modelled as a plane parallel circular source with energy spectra representing reference medium energy x-ray beam qualities at National Physical Laboratory (NPL) corresponding to 0.5, 1, 2 and 4 mm of Cu HVL (table 1) (Bass *et al* 2019). The MC model of the x-ray source and the calculation geometry was validated against a set of measurements carried out in a water phantom. The data are not presented in this manuscript.

The setup was modelled as a 30 × 30 cm^2 (in transverse direction) water phantom at SSD of 30 cm with thickness varying between 200 μm and 30 cm. The dose was scored in a small cylindrical scoring volume (200 μm diameter, 200 μm height) with its centre positioned at 100 μm depth from the front face of the water phantom (figure 1) to retrieve the correction factors associated with lack of full backscatter conditions.

In order to derive the backscatter correction factor, f_w, (required to correct for lack of full backscatter conditions) for dose to water determination at the surface of the phantom, dose calculated in the scoring volume at 100 μm depth, $D^t_{w,z=100\mu m}$, was plotted as a function of thicknesses of underlying water and extrapolated to zero thickness using a fitting function. The statistical uncertainty of calculated $D^t_{w,z=100\mu m}$ was below 0.2%.The intercept with the vertical axis gives $D^{t=0}_{w,z=0}$, where t indicates the overall thickness of the phantom, w is the phantom material (i.e. water) and z is the depth at which the dose is calculated. The calculations were carried out for a range of different field sizes, ϕ, ranging from 1 cm to 30 cm diameter. The backscatter correction factor (f_w), was calculated as a quotient of two difference terms represented by equation (3):

$$f_w(\phi, HVL, t) = \frac{D^t_{w,z=100\mu m} - D^{t=0}_{w,z=0}}{D^{t=30cm}_{w,z=100\mu m} - D^{t=0}_{w,z=0}}(\phi, HVL), \tag{3}$$

where the top term represents dose at the phantom surface ($z = 0$) for thickness t of underlying water and the bottom term is the surface dose for the full backscatter condition (i.e. for $t = 30\,cm$). f_w is dependent on the filed size, HVL and thickness of underlying water.

The factor f_w allows to correct the expression for the absorbed dose to water at the surface of the phantom when using the in-air method (given in equation (1)) for lack of full backscatter conditions using the following relation:

$$D^{t}_{w,z=0} = MN_K\left[1 + (B_w - 1)\, f_w\right]\left[\left(\frac{\bar{\mu}_{en}}{\rho}\right)^{water}_{air}\right]_{air}. \tag{4}$$

For the extreme cases, when $t \to 0$ (no backscatter phantom) $f_w \to 0$, equation (4) becomes the expression for a water kerma free in air. When the full backscatter conditions are fulfilled, i.e. $f_w \to 1$, equation (10) is becoming a classical dose to water expression determined at the surface of the phantom (i.e. equation (1)).

2.3. Validation of the Monte Carlo model based on measurements at 2 cm depth, $D_{w,z=2}$

The impact of partial backscatter on absorbed dose measurements at 2 cm depth has been assessed using EGSnrc, as described above. This step allows for validation of the model described against the experimental data. The MC setup is represented in figure 1, however, in this case the scoring volume has been placed at 2 cm depth. The Monte Carlo model was validated against a set of measurements, carried out with a PTW 30 012 ionization chamber, for 10, 15, 20 and 30 cm beam diameter for all beam qualities investigated in this work, given in table 1. The measurements have been carried out by changing the thickness of underlying water material behind the chamber in steps of 1 cm (up to 10 cm depth) and then in 5 cm steps up to depth of 30 cm. The chamber geometry has not been modelled for the MC calculations and it was assumed that k_{ch} factor does not vary with the backscatter thickness. The relative dose reduction (RDR_w) at 2 cm depth due to lack of full backscatter conditions has been calculated as

$$RDR_w\left(\phi, HVL, t\right) = \frac{D^{t}_{w,z=2}}{D^{t=30cm}_{w,z=2}}\left(\phi, HVL\right), \tag{5}$$

where $D^{t}_{w,z=2}$ is the dose at the depth of 2 cm for thickness t of underlying water and $D^{t=30cm}_{w,z=2}$ is the dose for the full backscatter condition. RDR_w is dependent on the field size, HVL and thickness of underlying water.

2.4. Determination of relative depth dose profiles with reduced backscatter material

Mote Carlo calculations, described in section 2.1 allowed to generate relative depth dose (RDD) profiles for all beam qualities investigated in this work for a thickness of underlying material, t, ranging from 1 mm to 30 cm. The data sets were simulated for a number of beam diameters, ϕ, spanning from 1 cm to 30 cm. Relative depth dose profiles were calculated as a ratio of doses scored along the beam's central axis $D_{w,z}$ normalized for the dose at 1 mm depth, $D_{w,z=1mm}$,

$$RDD_{z=1mm}\left(\phi, HVL, t\right) = \frac{D_{w,z}}{D_{w,z=1mm}}\left(\phi, HVL, t\right). \tag{6}$$

3. Results

3.1. Field size and HVL dependence of the backscatter correction factor

The dependence of the backscatter correction factor on the thickness of underlying water is given in figure 2 for selected beam sizes and HVLs. The full backscatter correction factor (f) increases with the amount of material available for scattering. For the full scatter conditions, i.e. $t = 30\,cm$, the f_w factor is a unity for a given HVL and field size and is equal to 0 when thickness of the underlying material tends to 0. Specimens placed on thin supporting shelves (< 1 cm) can be affected by a significantly (< 95%) reduced backscatter factor compared to reference conditions and this should be considered when calculating dose in pre-clinical radiotherapy.

The f_w curves rise quickly for small field sizes and the initial steepness becomes shallower with increasing field size. This was found to hold true for all beam qualities. The initial slope of f_w curves decreases with increasing beam hardness, that is, with the HVL of the radiation beam. The amount of underlying material necessary to produce maximum backscatter increases with beam quality.

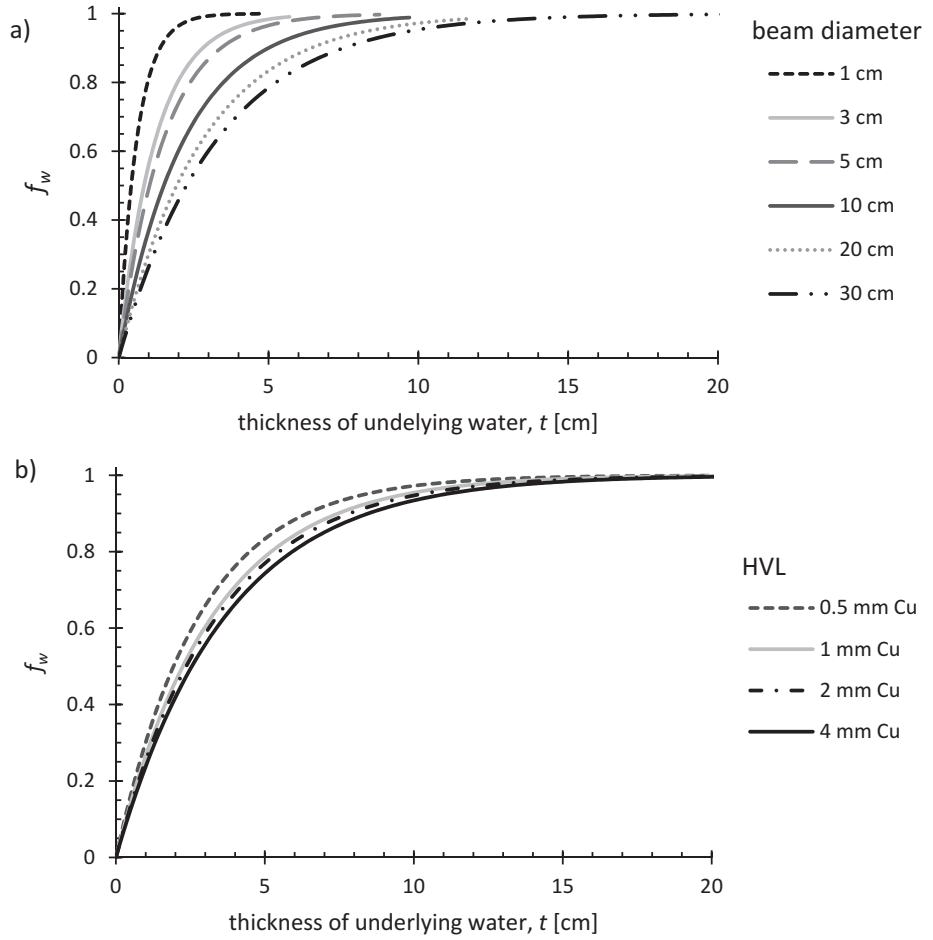

Figure 2. (a) Dependence of the backscatter build-up for 0.5 mm HVL on thickness of underlying material, t, and the field size. (b) Dependence of the backscatter build-up (f_w) on radiation beam quality for 20 cm diameter field size.

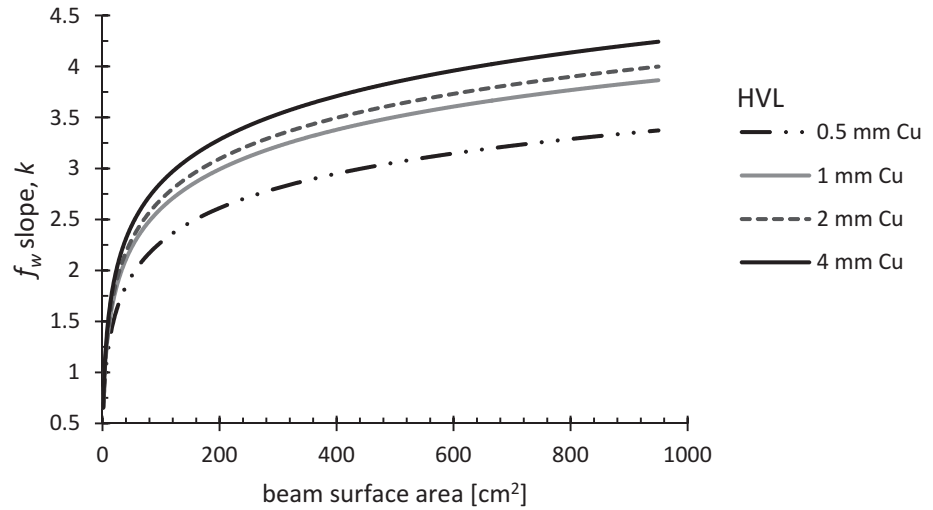

Figure 3. Dependence of reciprocal of the slope, k, of the backscatter correction factor on radiation beam quality and beam surface area.

The curves in figure 2 represent the best fit to the MC-calculated data used to calculate f_w based on equation (3). The dependence of the f_w on material thickness, beam area and beam quality, can be expressed by the following exponential relationship:

$$f_w(t) = 1 - exp\left(-\frac{t}{k}\right), \tag{7}$$

Table 2. Values of the constants a_1 and a_2 determined for the investigated beam qualities.

HVL [mm Cu]	a_1	a_2
0.5	2.033	2.785
1	1.775	2.212
2	1.715	2.156
4	1.617	1.881

where $f_w(t)$is the backscatter correction factor, t is the thickness of the underlying water in cm and k is a constant which describes the speed of rise, and hence the initial slope, of the f_w curves. This relationship has been previously used and validated by Klevenhagen for the low energy x-ray beams ranging from 1 mm up to 8 mm of Al HVL (Klevenhagen 1982) and it fits the data in this manuscript well.

To find a correlation of more general nature between the parameters which influence $f_w(t)$, the quantity k was determined for all field sizes and HVL involved in this work. These data are shown in figure 3. It is seen that k varies smoothly with beam size and can be correlated to the beam size for all beam qualities with the following expression:

$$k = \frac{1}{a_1} \cdot ln(A + a_2), \tag{8}$$

where k is the reciprocal of the initial slope of the $f_w(t)$ curves, a_1 and a_2 are constants dependent on beam quality (i.e. HVL) and A is the beam surface area in cm^2. Table 2 gives the constants a_1 and a_2 determined for beam qualities involved in this study.

For any other beam qualities, the initial slope, k, may be obtained from relationships between the constants a_1, and a_2 and the radiation quality, HVL, determined on the basis of the data given in figure 3. The relationship between constant a_1, a_2 and the HVL were found to fit the following equations:

$$a_1 = 1.65 + 0.99 \cdot \exp\left(-\frac{HVL}{0.53}\right), \tag{9}$$

$$a_2 = 1.98 + 2.21 \cdot \exp\left(-\frac{HVL}{0.49}\right), \tag{10}$$

In all equations, the HVL should be expressed in mm of Cu. These phenomenological expressions allow to retrieve the factor f_w for any beam quality between 0.5 and 4 mm Cu to correct for lack of full backscatter conditions in pre-clinical irradiators.

3.2. The effect of lack of backscatter on $D_{w,z=2}$

With regards to the in-phantom dosimetry approach, which is used for validation of the MC model presented in section 3.1, figure 4 shows the relative dose reduction at 2 cm depth due to lack of full backscatter conditions for all beam qualities investigated in this work.

The relative dose reduction factor decreases with the beam quality and becomes the most pronounced for the largest field sizes. The graphs in figure 4 allow determining the minimum thickness of backscatter material needed to fulfil the full backscatter conditions for the in-phantom method for all HVLs and field sizes used in this work. To enable readability of the graphs presented in figure 4, only experimental data for 10 cm and 30 cm diameter field size have been included. However, the agreement between measured and calculated data is very good for all of the field sizes used, indicating that field size and backscatter have negligible impact on k_{ch}. 10 cm of backscatter material is sufficient to fulfil the full-scatter conditions for x-ray beam with 0.5 mm Cu HVL and 10 cm diameter, however for harder beams such as 4 mm Cu HVL, at least 20 cm of underlying water is required. Small size beams are much less affected by the amount of backscatter material and 1 cm of additional backscatter is adequate for a 1 cm diameter beam.

3.3. Depth dose profiles for non-full scatter conditions

Figure 5 demonstrates the effect of the lack of full backscatter conditions on the relative depth dose profiles (i.e. Percentage Dose Depth—PDD) for 0.5 mm Cu HVL x-ray, 10 cm diameter beam. For better readability of figure 5, only data for five different backscatter thicknesses of water were plotted. The complete data sets for all beam qualities and all investigated beam diameters, spanning from 1 cm to 30 cm, are given in appendix 1. Reference depth dose profile for 0.5 mm of Cu HVL, 12 cm × 12 cm square field (British Institute of R, Institute of P, Engineering in M and Biology 1996) (corresponding to 10.6 cm diameter

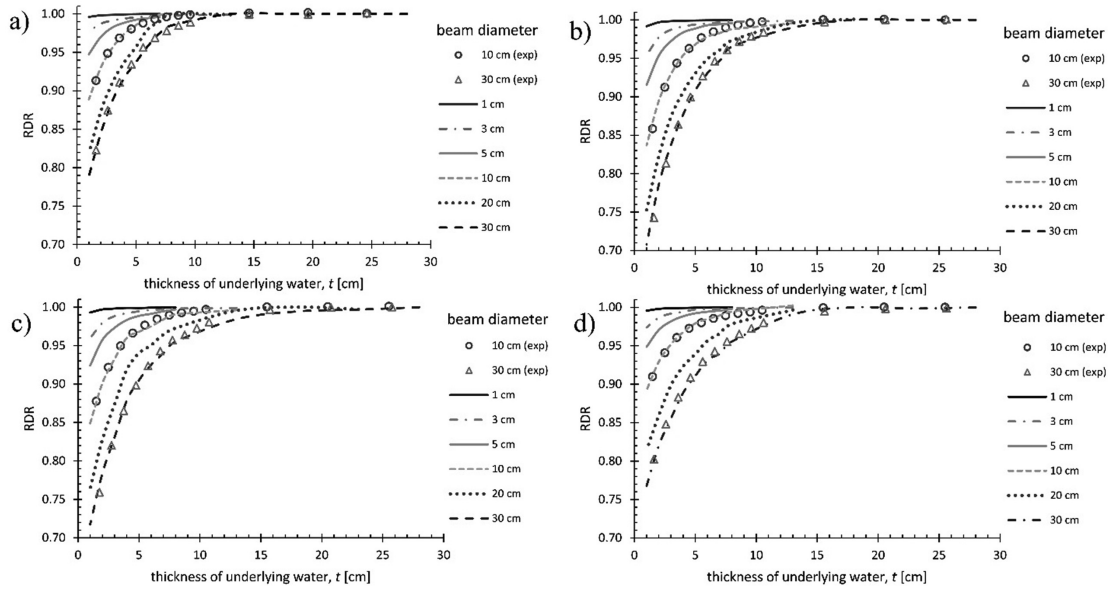

Figure 4. RDR as a function of thickness, t, of underlying water for (a) 0.5 mm Cu, (b) 1 mm Cu, (c) 2 mm Cu and (d) 4 mm Cu HVL. The RDR has been evaluated for beam diameters ranging from 1 cm up to 30 cm. The open circles and open triangles represent experimental data for 10 cm and 30 cm beam diameter, respectively.

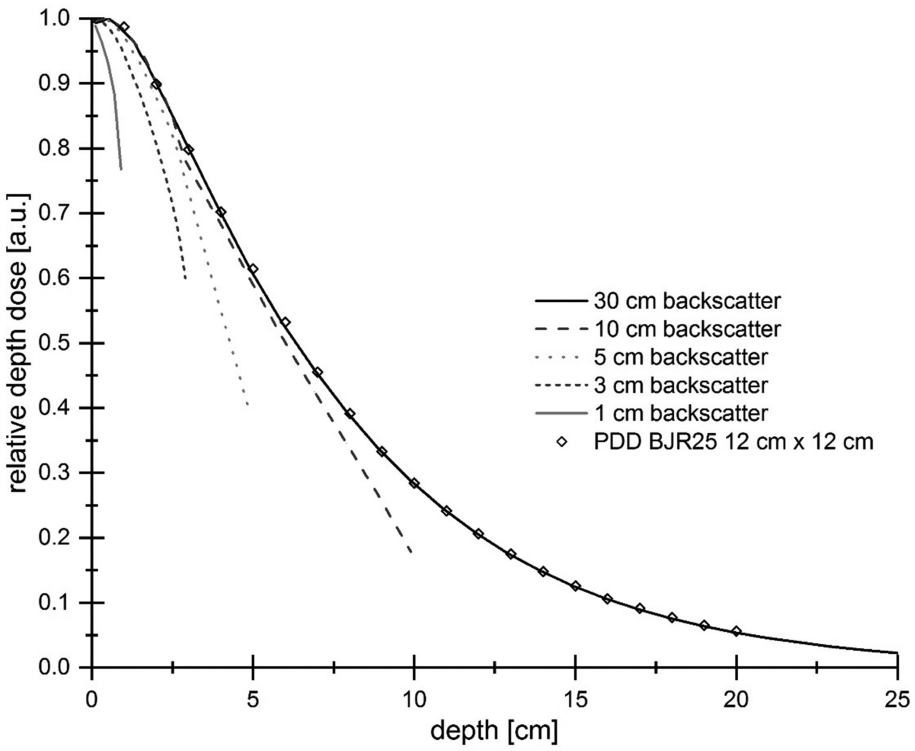

Figure 5. Relative depth dose profiles for different thickness of underlying water. Beam parameters: 0.5 mm Cu HVL, 10 cm diameter field size. Reference PDD from BJR Supplement 25 (Aird EGA, Radiology BIo, Physics Io, Medicine Ei and Biology 1996) for 12 × 12 cm^2 square field is included for comparison.

circular field) was added for comparison. The dose fall-off becomes steeper with decreasing thickness of water due to lack of backscattering. This effect is more prominent at large field sizes. The PDD data sets included in appendix 1 allow to retrieve the relative factor for determination of dose at any depth of interest for a given field size of NPL's reference medium energy x-rays radiation qualities.

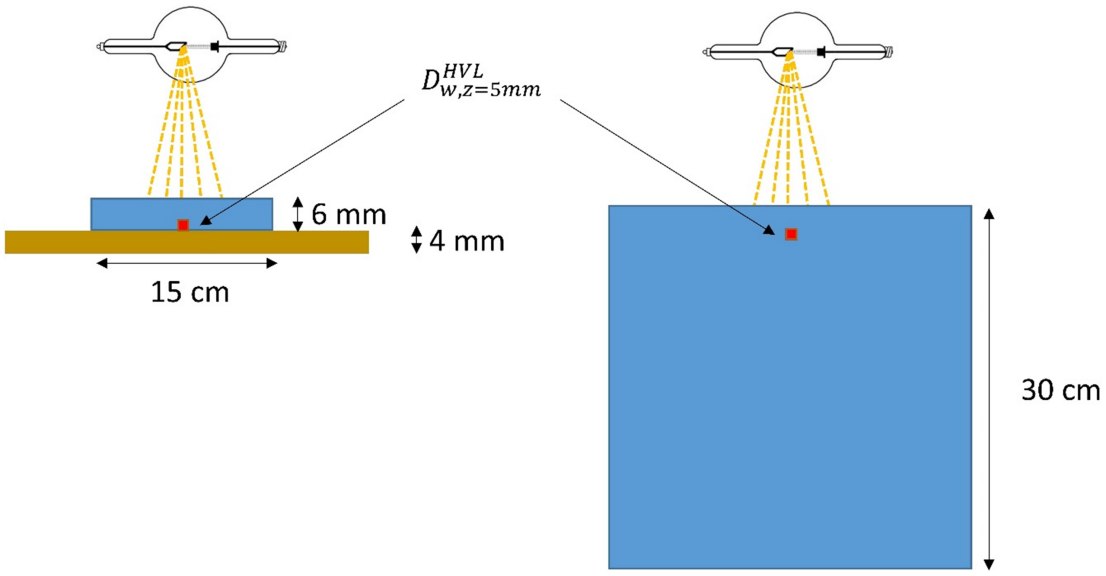

Figure 6. Illustration of the dosimetric impact of lack of full backscatter conditions in in vitro experiments: Petri Dish configuration (left) against reference conditions recommended by the CoP (right). Note: the dimensions are not to scale.

Table 3. The calculated underestimation of dose in 15 cm dimeter Petri Dish configuration with respect to full scatter conditions.

HVL [mm Cu]	δ [%]
0.5	43.1
1	38.2
2	35.9
4	27.1

3.4. Case study

To demonstrate the impact of lack of full backscatter in *in vitro* experiments, the dose absorbed by samples in a Petri Dish positioned on a 4 mm thick aluminium shelf (figure 6) has been compared to that calculated assuming full backscatter configuration, as recommended by the CoP (Klevenhagen *et al* 1996, Ma *et al* 2001, Aukett *et al* 2005). The dose deposited has been scored at 5 mm depth, $D^{HVL}_{w,z=5mm}$, for different HVLs investigated in this work. The Petri Dish has been modelled as 15 cm diameter 6 mm height cylinder filled with water. The dose underestimation factor, δ, of the Petri Dish configuration with respect to full scatter phantom conditions has been calculated as:

$$\delta\,(HVL) = 1 - \left(\frac{{}^{full\,scatter}D^{HVL}_{w,z=5mm}}{{}^{Petri\,Dish}D^{HVL}_{w,z=5mm}} \right), \tag{11}$$

where ${}^{full\,scatter}D^{HVL}_{w,z=5mm}$ is the dose scored at 5 mm depth in full backscatter phantom and ${}^{Petri\,Dish}D^{HVL}_{w,z=5mm}$ is dose calculated at 5 mm depth in Petri Dish positioned on a 4 mm thick aluminium shelf.

The effect of dose underestimation in the Petri Dish configuration in comparison to full backscatter phantom has been quantified for 30 cm beam diameter and beam qualities of 0.5, 1, 2 and 4 mm Cu HVL. The data are given in table 3.

3.5. Comparison with previously published data

To contrast our approach with previously published work by Chen *et al* (2019) we generated f_w values using equations (7)–(10) and calculated B'_w as a function of thickness of underlying water (shown in figure 7) for specific conditions investigated by Chen, i.e. 0.66 mm Cu HVL, square fields sizes ranging from 1 to 20 cm and SSD of 50 cm. Table V from AAPM TG-61 (Ma *et al* 2001) was used to interpolate B_w factors for full backscatter conditions for each of the square fields investigated by Chen *et al* (2019). All of the square fields have been converted to circular fields in order to accurately interpolate the B_w factors.

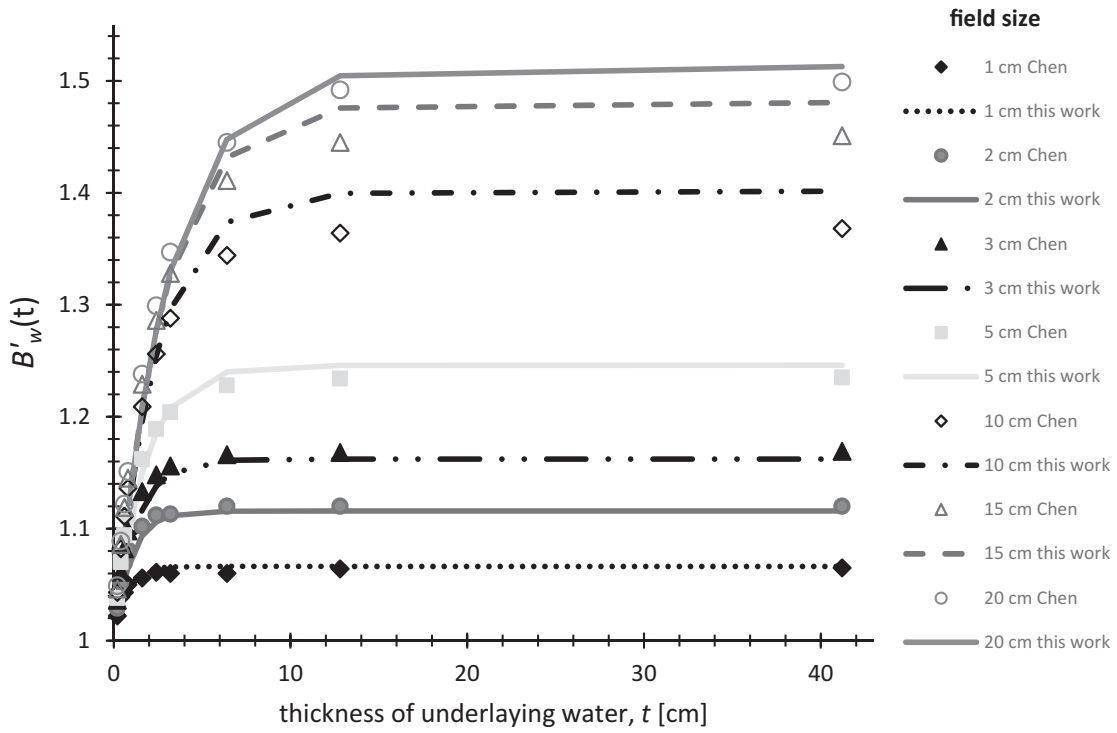

Figure 7. Comparison of $B'_w(t)$ values calculated by Chen (open and solid symbols) and based on the approach introduced in this work (lines). The indicated field sizes in the legend are given for the square fields.

4. Discussion

The dosimetry in orthovoltage x-ray units is strongly affected by the geometry of the experimental setup. The limiting factor in the pre-clinical units is the size and geometry of the irradiators which restrain the user from carrying out measurements in full scatter conditions as recommended by the relevant CoPs (Klevenhagen *et al* 1996, Ma *et al* 2001, Aukett *et al* 2005). Specifically, the thickness of the support shelf on which the specimens are placed and the size of the specimens themselves play a crucial role in the dose absorbed and it needs to be taken into account for accurate dosimetry. It is also important to appreciate that the backscatter material plays a critical role and it can significantly alter the dose absorbed by the biological samples (Kegel *et al* 2007). This work is based on water equivalent backscatter material which should be used as support for the biological samples when possible. If this is not feasible, the user should evaluate the additional dose contribution through appropriate simulation or experimental investigations. As shown in table 2 dose underestimations due to lack of full scatter conditions are well above the 5% uncertainty limit recommended by ICRU (1976) and due to their systematic nature, they would significantly alter the outcome of conventional *in vitro* studies (Dos Santos *et al* 2018). Clonogenic assay is the gold standard for radiation biology studies and the measured probability of cells surviving the radiation damage is assessed against the absorbed dose. This is generally quantified by calculating the α and β parameters from the linear quadratic model:

$$SF = e^{-\alpha D - \beta D^2}, \tag{12}$$

where SF is the surviving fraction measured and D is the dose absorbed. Any underestimation of the dose absorbed by the cells will, therefore, directly affect the values of the α and β parameters. Specifically, the α parameter will be underestimated by the same amount of the dose whilst the β parameter will be underestimated by the square of the dose underestimation factor. This would be more than a factor of 3 for the 0.5 mm Cu example reported here making direct comparison with similar experiments challenging. As the α/β ratio is used as index for the intrinsic radio-sensitivity of a cell line, incorrect dosimetry could alter the outcome of the study. Low α/β values (1.5–5 Gy) are normally associated with late responding tissues and indicate that radiation damage should be greatly spared by the use of dose fractions. By contrast the high α/β values (6–14 Gy) are observed for acutely responding tissues and indicate that the response is relatively

linear over the dose range of clinical interest. Dose underestimation in pre-clinical investigation of the order reported in table 3 could, therefore, easily lead to the incorrect classification of a late responding tissue with an α/β ratio of ~4 Gy as an acutely responding tissue.

Furthermore, the majority of *in vitro* cell survival measurements are used to assess the effectiveness of alternative radiation modalities or combinatory approaches. For charged particles, a parameter of clinical interest is the Relative Biological Effectiveness (RBE) defined as the ratio of x-ray and charged particle doses causing the same biological effect, which depends on type of radiation, dose delivered and biological endpoint. As the above discussed dosimetry issues will only affect the x-ray survival curves when kV x-ray beams are used (different protocols are employed for charged particle dosimetry and ^{60}Co irradiations and they are essentially the same for clinical and pre-clinical exposures), the potential dose underestimation of table 3 would cause an underestimation of the RBE by 73% to 57%. These are significant differences considering that the RBE for proton beams varies by less than 30% (from entrance to end of range) and RBE for heavier ions peaks at ~3.

The dose underestimation reported in table 3 will also alter the outcomes of drug-radiation combinatory studies even if the same experimental setup is used due to the non-linearity of the survival curves. For radio-sensitization studies (such as use of high-Z nanoparticles), the ratio of cell surviving fractions with/without radiosensitizer at a given dose (i.e. 2 Gy) termed as Radiation Enhancement Ratio (RER) is generally used as key parameter (Subiel *et al* 2016). Depending on the intrinsic radio-sensitivity of the cell line used for the study and the radio-sensitization effectiveness of the tested compound, dosimetry underestimation will result in significant underestimation of the radiation + compound effect potentially missing interesting translational opportunities. For low radio-sensitization effects (i.e. expected RER ~1.1), the dose underestimation of table 3 will result in 3%–7% underestimation of the REI whilst for compounds with high radio-sensitization potentials (i.e. expected RER ~1.4), the calculated RER would be underestimated by up to 26%.

Contrary to MV x-ray dosimetry, where the forward scattering effect is dominant, in orthovoltage photon beams large contributions to the absorbed dose to a point are due to backscattered radiation. These effects are clearly shown in figures 2 and 4 representing the effect of lack of full scatter conditions on the reduction of $D_{w,z=0}$ and $D_{w,z=2}$, respectively.

Equation (7) allows calculation of the backscatter correction factor, f_w, to be used as shown in equation (4) to calculate the absorbed dose to water at the surface using the in-air method in case of lack of full scatter conditions. The data reported also allows the calculation of the adequate thickness of the experimental setup in case the in-phantom dosimetry approach is to be followed to estimate the dose at 2 cm depth.

If the dose at a depth different from surface or 2 cm depth is required, the tabulated percentage depth dose profiles from appendix 1 can be used to correct for the beam attenuation or build-up at the relevant position in a specimen.

It is important to emphasize that B_w-values depend mainly on the x-ray spectrum, which can be characterized by its HVL, and the field size (Ma *et al* 2001, Andreo *et al* 2004). However, some dependence on the SSD, influencing beam divergence (Grosswendt 1990, 1993) and the peak tube voltage (Harrison 1982) has also been reported. The direct measurement of the primary and/or scattered x-ray beam spectra is difficult and requires specialist equipment, but can be estimated with software such as SpekCalc (Poludniowski 2007, Poludniowski and Evans 2007). However, as pointed out by Chica *et al* (2008) specifying the generating tube potential and homogeneity coefficient could be used together with HVL to characterize the beam quality more accurately. To date, the available dosimetry protocols still use only HVL as a beam quality specifier. More recently, Andreo (2019) published a comprehensive data set for low and medium energy x-ray beams, where relevant dosimetric factors, including B_w have been tabulated as a function of HVL and tube voltage potential. Andreo pointed out that for a given HVL and field size the variation of B_w can be up to 5%, however this statement is applicable to low energy x-rays (HVL below 0.5 mm Cu), which are not considered in this work. B_w for higher beam qualities have not been published by Andreo. In terms of SSD, as pointed out by Grosswendt (Grosswendt 1990), for higher beam qualities with larger field sizes a change in B_w can be noticeable. For instance, when changing SSD from 30 to 50 cm, the backscatter factor will increase by 1.4% for a beam with 4 mm Cu HVL and 20 cm diameter. This effect becomes more pronounced with decreasing energy. In pre-clinical irradiators SSD typically varies between 30 and 60 cm, hence if larger field sizes are used, the difference in B_w factor should be corrected or accounted for in the uncertainty budget. Beams with smaller field sizes, i.e. with 5 cm diameter and HVLs investigated in this work do not require significant correction due to change in SSD as B_w factor variations are below 0.5%. It is also worth noting that the CoP estimates the uncertainty of B_w at 3% (for $k = 2$).

Figure 7 provides a comparison between previously published $B'_w(t)$ factors (Chen *et al* 2019) and fractional backscatter factors calculated using the approach described in this work for 0.66 mm Cu HVL. The figure shows a reasonably good agreement for most of the field sizes, however there is some discrepancy (approx. 2–2.5% difference) for 10 and 15 cm fields. This could be attributed to over 2% difference between B_w factors calculated by Chen and the factors interpolated from AAPM TG-61 protocol. For instance, the interpolated B_w factor for 11.3 cm diameter (equivalent to 10 cm square) beam for SSD of 50 cm is equal to 1.401, while Chen's factor equates to 1.368 for full backscatter condition. Another reason could be difference in SSD between this work and Chen's study. In general, this comparison shows that the approach to correct the full backscatter factor B_w using f_w is robust and can be applied in a wide range of medium energy x-ray beams using only HVL as beam quality specifier. However, it is worth to remind that this approach is not perfect and uncertainties should be always be assigned when determining D_w for a particular irradiation conditions.

A final key question concerns the use of the in-phantom method when full backscattering conditions are not satisfied. The Monte Carlo and experimental data presented in section 3.2 suggests that variation in k_{ch} correction factor, given in equation (2), is negligible with changing thickness of backscatter material. A critical review of equation (2) points also to the $\left[\left(\frac{\bar{\mu}_{en}}{\rho}\right)_{air}^{water}\right]_{z=2,\phi}$ factor which could depend on the specific scattering conditions as these will affect the spectral distribution of the beam. This influence has not been previously investigated, however based on work published by Knight and Nahum (1994) it is possible to approximately estimate the effect of the potential change in the ratio of mass energy absorption coefficient water to air factor. The authors reported the $\left[\left(\frac{\bar{\mu}_{en}}{\rho}\right)_{air}^{water}\right]_{z=2,\phi}$ factor for 0.45, 1.7 and 3 mm Cu HVL beams of 11.2 cm diameter as a function of the depth in water. This study has shown that for the softer medium energy x-ray beam investigated (0.45 mm Cu), the ratio of mass energy absorption coefficient water to air varied by less than 0.5% in the 0 to 10 cm depth range in a water. For the harder beam (3 mm Cu), the maximum variation observed was 1%. Knight's work indicates that the in-phantom method and equation (2) could still be used for the determination of $D_{w,z=2}$ in the case of lack of full backscatter conditions providing that larger uncertainties are adopted for the ratio of mass energy absorption coefficient ratio water to air factor. It is, however, important to evaluate the accurate $\left[\left(\frac{\bar{\mu}_{en}}{\rho}\right)_{air}^{water}\right]_{z=2,\phi}$ values in the case of reduced backscattered conditions and publish them in the future code of practice for pre-clinical orthovoltage irradiations.

5. Conclusions

The main focus of this work was to evaluate the effects of the lack of recommended reference conditions in dosimetry measurements for pre-clinical settings. The analytical expressions derived provide the user community with an approach to correct the in-air CoP recommended measurements for specific experimental conditions using backscatter correction factors. Similarly, the data reported allow to identify the experimental set up for which the in-phantom dosimetry method can be adopted with confidence. Finally, the tabulated percentage depth dose profiles provided in appendix 1 allow for the determination of absorbed dose at different depths than 0 and 2 cm. This work is aimed at extending the recommendations of the current CoPs (Klevenhagen *et al* 1996, Ma *et al* 2001) to practical experimental conditions and highlighting the potential impact of the lack of correct backscatter considerations on radiobiological studies such as assessment of alpha/beta ratios and RBE investigations. It is clear that codes of practice for dosimetry in radiobiology should be updated or redefined to better address experimental conditions in pre-clinical x-ray units.

Acknowledgments

This work was supported by Innovate UK Grant No. 102524.

Appendix 1

Table A1. Percentage depth dose depositions for different phantom thickness and field sizes for (a) 0.5 mm Cu, (b) 1 mm Cu, (c) 2 mm Cu and (d) 4 mm Cu HVL.

(a)

		thickness of backscatter material [cm]												
field size diameter [cm]	depth [cm]	30	20	15	10	9	8	7	6	5	4	3	2	1
1	*0.1*	1.00	1.00	1.00	1.00	1.00	1.00	1.00	1.00	1.00	1.00	1.00	1.00	1.00
	0.3	0.96	0.96	0.96	0.96	0.96	0.96	0.96	0.96	0.96	0.96	0.96	0.96	0.95
	0.5	0.93	0.93	0.93	0.93	0.93	0.93	0.93	0.93	0.93	0.93	0.93	0.93	0.91
	0.7	0.90	0.90	0.90	0.90	0.90	0.90	0.90	0.90	0.90	0.90	0.89	0.89	0.86
	0.9	0.86	0.86	0.86	0.86	0.86	0.86	0.86	0.86	0.86	0.86	0.86	0.86	0.68
	1.1	0.83	0.83	0.83	0.83	0.83	0.83	0.83	0.83	0.83	0.83	0.83	0.82	
	1.3	0.80	0.80	0.80	0.80	0.80	0.80	0.80	0.80	0.80	0.80	0.80	0.79	
	1.5	0.77	0.77	0.77	0.77	0.77	0.77	0.77	0.77	0.77	0.77	0.77	0.75	
	1.7	0.74	0.74	0.74	0.74	0.74	0.74	0.74	0.74	0.74	0.74	0.73	0.71	
	2	0.71	0.71	0.71	0.71	0.71	0.71	0.71	0.71	0.71	0.71	0.70	0.58	
	3	0.54	0.54	0.54	0.54	0.54	0.54	0.54	0.54	0.54	0.53	0.44		
	4	0.44	0.44	0.44	0.44	0.44	0.44	0.44	0.44	0.43	0.38			
	5	0.36	0.36	0.36	0.36	0.36	0.36	0.36	0.35	0.28				
	6	0.29	0.29	0.29	0.29	0.29	0.29	0.29	0.29					
	7	0.24	0.24	0.24	0.24	0.24	0.24	0.20						
	8	0.20	0.20	0.20	0.20	0.19	0.18							
	9	0.16	0.16	0.16	0.16	0.14								
	10	0.13	0.13	0.13	0.09									
	15	0.05	0.05	0.03										
	20	0.02	0.01											
5	*0.1*	1.00	1.00	1.00	1.00	1.00	1.00	1.00	1.00	1.00	1.00	1.00	1.00	1.00
	0.3	1.00	1.00	1.00	1.00	1.00	1.00	0.99	0.99	0.99	0.99	0.99	0.99	0.96
	0.5	0.99	0.99	0.99	0.99	0.99	0.99	0.99	0.98	0.99	0.98	0.98	0.97	0.93
	0.7	0.97	0.97	0.97	0.97	0.97	0.97	0.97	0.97	0.97	0.97	0.96	0.94	0.88
	0.9	0.96	0.96	0.96	0.96	0.96	0.96	0.96	0.95	0.95	0.95	0.94	0.91	0.72
	1.1	0.94	0.94	0.94	0.94	0.94	0.94	0.94	0.93	0.93	0.93	0.91	0.88	
	1.3	0.92	0.92	0.92	0.92	0.92	0.92	0.92	0.91	0.91	0.90	0.89	0.85	
	1.5	0.90	0.90	0.90	0.90	0.90	0.90	0.91	0.89	0.89	0.88	0.86	0.80	
	1.7	0.88	0.88	0.88	0.88	0.88	0.87	0.87	0.87	0.86	0.85	0.83	0.75	
	2	0.86	0.86	0.85	0.85	0.85	0.85	0.85	0.85	0.84	0.83	0.80	0.62	
	3	0.70	0.70	0.70	0.69	0.69	0.69	0.68	0.67	0.66	0.61	0.49		
	4	0.59	0.59	0.59	0.59	0.59	0.58	0.57	0.56	0.52	0.41			
	5	0.50	0.50	0.50	0.49	0.49	0.48	0.45	0.43	0.34				
	6	0.42	0.42	0.42	0.41	0.41	0.39	0.33	0.28					
	7	0.35	0.35	0.35	0.34	0.33	0.30	0.24						
	8	0.30	0.30	0.29	0.27	0.25	0.20							
	9	0.25	0.25	0.24	0.21	0.17								
	10	0.21	0.21	0.20	0.14									
	15	0.08	0.08	0.06										
	20	0.03	0.02											
10	*0.1*	0.99	1.00	0.99	1.00	0.99	0.99	1.00	1.00	1.00	1.00	1.00	1.00	0.99
	0.3	1.00	1.00	1.00	1.00	1.00	1.00	1.00	1.00	1.00	1.00	1.00	0.99	0.96
	0.5	1.00	1.00	1.00	1.00	1.00	1.00	1.00	1.00	1.00	0.99	0.99	0.98	0.93
	0.7	0.99	0.99	1.00	0.99	0.99	0.99	0.99	0.99	0.99	0.98	0.97	0.95	0.88
	0.9	0.98	0.99	0.99	0.99	0.99	0.98	0.99	0.98	0.98	0.97	0.96	0.93	0.77
	1.1	0.97	0.98	0.98	0.98	0.97	0.97	0.98	0.97	0.96	0.95	0.93	0.90	
	1.3	0.96	0.96	0.97	0.96	0.96	0.96	0.96	0.95	0.95	0.93	0.91	0.86	
	1.5	0.95	0.96	0.95	0.95	0.95	0.95	0.94	0.94	0.93	0.91	0.88	0.82	
	1.7	0.94	0.94	0.94	0.93	0.93	0.93	0.93	0.92	0.91	0.89	0.85	0.77	
	2	0.92	0.92	0.92	0.92	0.92	0.91	0.91	0.90	0.89	0.86	0.82	0.66	
	3	0.80	0.80	0.80	0.79	0.78	0.78	0.77	0.75	0.72	0.65	0.54		
	4	0.70	0.70	0.70	0.69	0.69	0.68	0.66	0.63	0.57	0.47			
	5	0.61	0.61	0.61	0.60	0.59	0.57	0.54	0.49	0.39				
	6	0.53	0.53	0.53	0.51	0.49	0.47	0.42	0.34					
	7	0.46	0.46	0.46	0.43	0.40	0.36	0.29						
	8	0.39	0.39	0.39	0.35	0.31	0.26							
	9	0.34	0.34	0.33	0.26	0.21								

(Continued)

Table A1. (Continued)

(a)

field size diameter [cm]	depth [cm]	thickness of backscatter material [cm]												
		30	20	15	10	9	8	7	6	5	4	3	2	1
10	0.29	0.29	0.28	0.18										
	15	0.13	0.12	0.08										
	20	0.05												
20	*0.1*	0.98	0.98	0.98	0.98	0.99	0.99	0.98	0.99	0.99	1.00	1.00	1.00	0.99
	0.3	0.98	0.99	0.99	0.99	0.99	0.99	0.99	1.00	1.00	1.00	1.00	0.99	0.97
	0.5	0.99	1.00	1.00	0.99	1.00	1.00	1.00	1.00	1.00	1.00	0.99	0.98	0.93
	0.7	1.00	1.00	1.00	1.00	1.00	1.00	1.00	1.00	0.99	0.99	0.98	0.96	0.88
	0.9	0.99	1.00	1.00	0.99	0.99	1.00	0.99	0.99	0.99	0.98	0.96	0.93	0.80
	1.1	0.99	1.00	1.00	0.99	1.00	0.99	0.99	0.98	0.98	0.97	0.94	0.90	
	1.3	0.98	0.99	0.99	0.99	0.99	0.99	0.98	0.98	0.96	0.95	0.92	0.86	
	1.5	0.98	0.98	0.98	0.97	0.98	0.98	0.96	0.96	0.95	0.93	0.89	0.82	
	1.7	0.97	0.98	0.97	0.96	0.97	0.96	0.95	0.95	0.93	0.91	0.87	0.77	
	2	0.96	0.97	0.96	0.95	0.95	0.95	0.94	0.93	0.91	0.89	0.84	0.69	
	3	0.87	0.87	0.87	0.85	0.85	0.84	0.82	0.79	0.76	0.68	0.57		
	4	0.79	0.80	0.80	0.77	0.76	0.75	0.71	0.67	0.60	0.50			
	5	0.72	0.72	0.72	0.68	0.67	0.64	0.60	0.53	0.43				
	6	0.64	0.65	0.64	0.59	0.57	0.54	0.47	0.40					
	7	0.57	0.57	0.56	0.51	0.48	0.42	0.33						
	8	0.51	0.51	0.50	0.42	0.37	0.30							
	9	0.44	0.45	0.43	0.32	0.27								
	10	0.39	0.39	0.37	0.22									
	15	0.19	0.18	0.10										
	20	0.09	0.05											
30	*0.1*	0.96	0.96	0.97	0.96	0.97	0.97	0.98	0.98	0.99	0.99	1.00	1.00	0.99
	0.3	0.98	0.98	0.99	0.98	0.98	0.99	0.99	0.99	0.99	1.00	1.00	0.99	0.97
	0.5	0.99	0.99	0.99	0.99	0.99	0.99	0.99	1.00	1.00	1.00	0.99	0.98	0.93
	0.7	1.00	1.00	0.99	1.00	1.00	1.00	1.00	0.99	0.99	0.99	0.98	0.95	0.88
	0.9	1.00	1.00	1.00	1.00	0.99	1.00	1.00	0.99	0.99	0.98	0.97	0.93	0.81
	1.1	0.99	0.99	1.00	0.99	0.99	0.99	0.99	0.98	0.98	0.96	0.95	0.91	
	1.3	1.00	0.99	0.99	0.98	0.98	0.99	0.98	0.97	0.96	0.95	0.92	0.86	
	1.5	0.99	0.99	0.99	0.97	0.98	0.97	0.97	0.96	0.95	0.93	0.90	0.82	
	1.7	0.98	0.99	0.98	0.97	0.96	0.96	0.96	0.95	0.94	0.91	0.87	0.78	
	2	0.98	0.98	0.98	0.95	0.96	0.95	0.95	0.93	0.92	0.89	0.84	0.69	
	3	0.90	0.90	0.90	0.87	0.86	0.85	0.83	0.80	0.76	0.68	0.59		
	4	0.83	0.83	0.83	0.79	0.78	0.76	0.73	0.69	0.61	0.56			
	5	0.76	0.76	0.76	0.71	0.69	0.67	0.62	0.54	0.46				
	6	0.69	0.69	0.68	0.62	0.60	0.55	0.49	0.39					
	7	0.62	0.62	0.61	0.54	0.50	0.44	0.35						
	8	0.56	0.55	0.54	0.44	0.39	0.35							
	9	0.50	0.50	0.48	0.34	0.28								
	10	0.44	0.44	0.41	0.23									
	15	0.24	0.22	0.13										
	20	0.12												

(b)

field size diameter [cm]	depth [cm]	thickness of backscatter material [cm]												
		30	20	15	10	9	8	7	6	5	4	3	2	1
1	*0.1*	1.00	1.00	1.00	1.00	1.00	1.00	1.00	1.00	1.00	1.00	1.00	1.00	1.00
	0.3	0.97	0.97	0.97	0.97	0.97	0.97	0.97	0.97	0.97	0.97	0.97	0.97	0.96
	0.5	0.94	0.94	0.94	0.94	0.94	0.94	0.94	0.94	0.94	0.94	0.94	0.94	0.93
	0.7	0.92	0.92	0.92	0.92	0.92	0.92	0.92	0.92	0.92	0.92	0.91	0.91	0.89
	0.9	0.89	0.89	0.89	0.89	0.89	0.89	0.89	0.89	0.89	0.89	0.89	0.88	0.73
	1.1	0.86	0.86	0.86	0.86	0.86	0.86	0.86	0.86	0.86	0.86	0.86	0.85	
	1.3	0.83	0.83	0.83	0.83	0.83	0.83	0.83	0.83	0.83	0.83	0.83	0.82	
	1.5	0.81	0.81	0.81	0.81	0.81	0.81	0.81	0.81	0.81	0.81	0.80	0.79	
	1.7	0.78	0.78	0.78	0.78	0.78	0.78	0.78	0.78	0.78	0.78	0.78	0.76	
	2	0.76	0.76	0.76	0.76	0.76	0.76	0.76	0.76	0.75	0.75	0.75	0.63	
	3	0.60	0.60	0.60	0.60	0.60	0.60	0.60	0.60	0.60	0.59	0.48		

(Continued)

Table A1. (Continued)

(b)

field size diameter [cm]	depth [cm]	thickness of backscatter material [cm]												
		30	20	15	10	9	8	7	6	5	4	3	2	1
	4	0.50	0.50	0.50	0.50	0.50	0.50	0.50	0.50	0.50	0.42			
	5	0.43	0.43	0.43	0.43	0.43	0.42	0.42	0.42	0.32				
	6	0.36	0.36	0.36	0.36	0.36	0.36	0.35	0.28					
	7	0.30	0.30	0.30	0.30	0.30	0.30	0.24						
	8	0.26	0.26	0.26	0.25	0.25	0.21							
	9	0.22	0.22	0.22	0.21	0.19								
	10	0.18	0.18	0.18	0.14									
	15	0.08	0.08	0.05										
	20	0.03	0.02											
5	*0.1*	1.00	1.00	1.00	1.00	1.00	1.00	1.00	1.00	1.00	1.00	1.00	1.00	1.00
	0.3	1.00	1.00	1.00	1.00	1.00	1.00	1.00	1.00	1.00	1.00	0.99	0.99	0.98
	0.5	0.99	0.99	0.99	0.99	0.99	0.99	0.99	0.99	0.99	0.99	0.98	0.98	0.95
	0.7	0.98	0.98	0.98	0.98	0.98	0.98	0.98	0.98	0.98	0.97	0.97	0.96	0.91
	0.9	0.97	0.97	0.97	0.97	0.97	0.97	0.97	0.97	0.96	0.96	0.95	0.93	0.76
	1.1	0.95	0.96	0.95	0.95	0.95	0.95	0.95	0.95	0.95	0.94	0.93	0.91	
	1.3	0.94	0.94	0.94	0.94	0.94	0.94	0.94	0.93	0.93	0.92	0.91	0.88	
	1.5	0.92	0.92	0.92	0.92	0.92	0.92	0.92	0.92	0.91	0.90	0.89	0.84	
	1.7	0.90	0.90	0.90	0.90	0.90	0.90	0.90	0.90	0.89	0.88	0.86	0.80	
	2	0.88	0.88	0.88	0.88	0.88	0.88	0.88	0.88	0.87	0.86	0.83	0.66	
	3	0.75	0.75	0.75	0.74	0.74	0.74	0.74	0.73	0.71	0.67	0.55		
	4	0.65	0.65	0.65	0.65	0.65	0.64	0.63	0.62	0.58	0.47			
	5	0.57	0.57	0.56	0.56	0.55	0.55	0.53	0.50	0.41				
	6	0.49	0.49	0.49	0.48	0.47	0.46	0.43	0.34					
	7	0.42	0.42	0.42	0.40	0.39	0.37	0.30						
	8	0.36	0.36	0.36	0.34	0.32	0.25							
	9	0.31	0.31	0.30	0.27	0.22								
	10	0.26	0.26	0.26	0.19									
	15	0.12	0.12	0.09										
	20	0.05	0.04											
10	*0.1*	0.99	0.99	0.99	0.99	0.99	0.99	0.99	1.00	1.00	1.00	1.00	1.00	1.00
	0.3	1.00	1.00	1.00	1.00	1.00	1.00	1.00	1.00	1.00	1.00	1.00	1.00	0.98
	0.5	1.00	1.00	1.00	1.00	1.00	1.00	1.00	1.00	1.00	1.00	0.99	0.98	0.95
	0.7	1.00	1.00	1.00	1.00	1.00	1.00	0.99	0.99	0.99	0.99	0.98	0.97	0.92
	0.9	0.99	0.99	0.99	0.99	0.99	0.99	0.99	0.99	0.98	0.98	0.97	0.94	0.80
	1.1	0.99	0.99	0.99	0.99	0.98	0.98	0.98	0.98	0.97	0.97	0.95	0.92	
	1.3	0.98	0.98	0.98	0.97	0.97	0.97	0.97	0.97	0.96	0.95	0.93	0.89	
	1.5	0.97	0.97	0.97	0.97	0.97	0.96	0.96	0.95	0.95	0.94	0.91	0.86	
	1.7	0.96	0.96	0.96	0.95	0.95	0.95	0.94	0.94	0.93	0.92	0.89	0.82	
	2	0.95	0.94	0.94	0.94	0.94	0.94	0.93	0.93	0.91	0.90	0.86	0.70	
	3	0.84	0.84	0.84	0.83	0.83	0.82	0.81	0.79	0.77	0.71	0.60		
	4	0.76	0.76	0.76	0.75	0.74	0.73	0.71	0.68	0.63	0.52			
	5	0.68	0.68	0.68	0.66	0.65	0.63	0.61	0.56	0.46				
	6	0.60	0.60	0.60	0.57	0.56	0.54	0.49	0.40					
	7	0.53	0.53	0.53	0.49	0.47	0.43	0.34						
	8	0.47	0.47	0.46	0.41	0.38	0.31							
	9	0.41	0.41	0.40	0.33	0.27								
	10	0.36	0.35	0.34	0.23									
	15	0.17	0.17	0.11										
	20	0.08	0.05											
20	*0.1*	0.97	0.97	0.97	0.98	0.98	0.98	0.98	0.99	0.99	0.99	1.00	1.00	1.00
	0.3	0.99	0.99	0.99	0.99	0.99	0.99	1.00	1.00	1.00	1.00	1.00	1.00	0.98
	0.5	1.00	1.00	0.99	1.00	1.00	1.00	1.00	1.00	1.00	1.00	1.00	0.98	0.95
	0.7	1.00	1.00	1.00	1.00	1.00	0.99	1.00	1.00	1.00	1.00	0.99	0.97	0.92
	0.9	1.00	1.00	1.00	1.00	1.00	1.00	1.00	1.00	0.99	0.99	0.97	0.95	0.81
	1.1	1.00	1.00	1.00	1.00	1.00	1.00	1.00	0.99	0.99	0.97	0.96	0.92	
	1.3	1.00	1.00	1.00	1.00	0.99	0.99	0.99	0.98	0.97	0.96	0.94	0.90	
	1.5	1.00	1.00	0.99	0.99	0.99	0.98	0.98	0.97	0.96	0.95	0.92	0.86	
	1.7	0.99	0.98	0.99	0.99	0.98	0.97	0.97	0.97	0.95	0.93	0.90	0.82	

(Continued)

Table A1. (Continued)

(b)

field size diameter [cm]	depth [cm]	thickness of backscatter material [cm]												
		30	20	15	10	9	8	7	6	5	4	3	2	1
	2	0.98	0.98	0.98	0.97	0.97	0.96	0.96	0.95	0.94	0.91	0.87	0.70	
	3	0.92	0.91	0.91	0.90	0.89	0.88	0.86	0.84	0.80	0.73	0.63		
	4	0.86	0.85	0.85	0.82	0.81	0.79	0.77	0.73	0.66	0.57			
	5	0.79	0.79	0.78	0.75	0.73	0.70	0.66	0.60	0.51				
	6	0.72	0.72	0.71	0.66	0.64	0.60	0.54	0.45					
	7	0.65	0.65	0.64	0.58	0.54	0.49	0.42						
	8	0.59	0.59	0.57	0.49	0.44	0.36							
	9	0.53	0.53	0.51	0.39	0.31								
	10	0.47	0.47	0.44	0.29									
	15	0.26	0.24	0.16										
	20	0.13	0.08											
30	*0.1*	0.93	0.96	0.96	0.97	0.97	0.97	0.98	0.98	0.99	0.98	1.00	1.00	1.00
	0.3	0.96	0.97	0.97	0.98	0.98	0.98	0.99	1.00	0.99	0.99	1.00	1.00	0.98
	0.5	0.97	0.98	0.98	0.99	1.00	0.99	1.00	1.00	1.00	1.00	0.99	0.99	0.95
	0.7	0.99	1.00	0.99	0.99	1.00	1.00	1.00	1.00	0.99	0.99	0.99	0.97	0.91
	0.9	1.00	0.99	0.99	1.00	1.00	0.99	1.00	1.00	0.99	0.98	0.98	0.95	0.85
	1.1	1.00	0.99	1.00	1.00	1.00	1.00	1.00	0.99	0.98	0.97	0.96	0.93	
	1.3	1.00	1.00	1.00	1.00	1.00	0.99	1.00	0.98	0.98	0.96	0.94	0.90	
	1.5	1.00	0.99	0.99	0.99	0.99	0.99	0.99	0.98	0.96	0.95	0.93	0.86	
	1.7	1.00	0.99	0.99	0.99	0.99	0.98	0.98	0.97	0.95	0.93	0.90	0.82	
	2	0.99	0.99	0.99	0.99	0.98	0.97	0.97	0.96	0.94	0.92	0.87	0.77	
	3	0.96	0.94	0.93	0.92	0.91	0.89	0.88	0.85	0.81	0.74	0.64		
	4	0.94	0.89	0.88	0.85	0.84	0.81	0.79	0.74	0.67	0.59			
	5	0.89	0.82	0.82	0.79	0.75	0.72	0.68	0.61	0.52				
	6	0.83	0.77	0.76	0.70	0.66	0.62	0.56	0.46					
	7	0.77	0.70	0.69	0.62	0.57	0.50	0.42						
	8	0.71	0.64	0.62	0.50	0.46	0.35							
	9	0.65	0.58	0.56	0.40	0.35								
	10	0.59	0.53	0.49	0.30									
	15	0.35	0.29	0.17										
	20	0.19	0.11											

(c)

field size diameter [cm]	depth [cm]	thickness of backscatter material [cm]												
		30	20	15	10	9	8	7	6	5	4	3	2	1
1	*0.1*	1.00	1.00	1.00	1.00	1.00	1.00	1.00	1.00	1.00	1.00	1.00	1.00	1.00
	0.3	0.97	0.97	0.97	0.97	0.97	0.97	0.97	0.97	0.97	0.97	0.97	0.97	0.97
	0.5	0.95	0.95	0.95	0.95	0.95	0.95	0.95	0.95	0.95	0.95	0.95	0.95	0.94
	0.7	0.92	0.92	0.92	0.92	0.92	0.92	0.92	0.92	0.92	0.92	0.92	0.92	0.90
	0.9	0.90	0.90	0.90	0.90	0.90	0.90	0.90	0.90	0.90	0.90	0.89	0.89	0.74
	1.1	0.87	0.87	0.87	0.87	0.87	0.87	0.87	0.87	0.87	0.87	0.87	0.86	
	1.3	0.84	0.84	0.84	0.84	0.84	0.84	0.84	0.84	0.84	0.84	0.84	0.84	
	1.5	0.82	0.82	0.82	0.82	0.82	0.82	0.82	0.82	0.82	0.82	0.82	0.81	
	1.7	0.79	0.79	0.79	0.79	0.79	0.79	0.79	0.79	0.79	0.79	0.79	0.77	
	2	0.77	0.77	0.77	0.77	0.77	0.77	0.77	0.77	0.77	0.77	0.76	0.64	
	3	0.62	0.62	0.62	0.62	0.62	0.62	0.62	0.62	0.61	0.61	0.47		
	4	0.53	0.53	0.53	0.52	0.52	0.52	0.52	0.52	0.52	0.44			
	5	0.45	0.45	0.45	0.45	0.45	0.45	0.45	0.44	0.35				
	6	0.38	0.38	0.38	0.38	0.38	0.38	0.38	0.33					
	7	0.32	0.32	0.32	0.32	0.32	0.32	0.29						
	8	0.28	0.28	0.28	0.27	0.27	0.22							
	9	0.24	0.24	0.24	0.23	0.19								
	10	0.20	0.20	0.20	0.15									
	15	0.09	0.09	0.05										
	20	0.04	0.02											

(Continued)

Table A1. (Continued)

(c)

field size diameter [cm]	depth [cm]	thickness of backscatter material [cm]												
		30	20	15	10	9	8	7	6	5	4	3	2	1
5	*0.1*	1.00	1.00	1.00	1.00	1.00	1.00	1.00	1.00	1.00	1.00	1.00	1.00	1.00
	0.3	1.00	1.00	1.00	1.00	1.00	1.00	1.00	1.00	1.00	1.00	0.99	0.99	0.99
	0.5	0.99	0.99	0.99	0.99	0.99	0.99	0.99	0.99	0.99	0.99	0.98	0.98	0.98
	0.7	0.98	0.98	0.98	0.98	0.98	0.98	0.98	0.98	0.98	0.98	0.97	0.96	0.96
	0.9	0.97	0.97	0.97	0.97	0.97	0.97	0.97	0.97	0.97	0.96	0.95	0.94	0.94
	1.1	0.96	0.96	0.96	0.96	0.96	0.96	0.95	0.95	0.95	0.95	0.94	0.92	
	1.3	0.94	0.94	0.94	0.94	0.94	0.94	0.94	0.94	0.93	0.93	0.92	0.89	
	1.5	0.93	0.93	0.93	0.92	0.93	0.92	0.92	0.92	0.92	0.91	0.90	0.86	
	1.7	0.91	0.91	0.91	0.91	0.91	0.91	0.90	0.90	0.90	0.89	0.87	0.82	
	2	0.89	0.89	0.89	0.89	0.89	0.89	0.89	0.88	0.88	0.87	0.85	0.67	
	3	0.76	0.76	0.76	0.76	0.75	0.75	0.75	0.74	0.73	0.69	0.57		
	4	0.67	0.67	0.67	0.66	0.66	0.66	0.65	0.64	0.61	0.49			
	5	0.58	0.58	0.58	0.58	0.57	0.57	0.55	0.53	0.42				
	6	0.51	0.51	0.51	0.50	0.49	0.48	0.45	0.37					
	7	0.44	0.44	0.44	0.43	0.42	0.39	0.32						
	8	0.38	0.38	0.38	0.36	0.34	0.27							
	9	0.33	0.33	0.32	0.29	0.24								
	10	0.28	0.28	0.28	0.20									
	15	0.13	0.13											
	20	0.06	0.05											
10	*0.1*	0.99	0.99	0.99	0.99	0.99	1.00	1.00	1.00	1.00	1.00	1.00	1.00	1.00
	0.3	1.00	1.00	1.00	1.00	1.00	1.00	1.00	1.00	1.00	1.00	1.00	0.99	0.98
	0.5	1.00	1.00	1.00	1.00	1.00	1.00	1.00	1.00	1.00	1.00	0.99	0.98	0.96
	0.7	1.00	1.00	1.00	1.00	1.00	1.00	1.00	1.00	0.99	0.99	0.98	0.97	0.92
	0.9	0.99	0.99	0.99	0.99	0.99	0.99	0.99	0.99	0.99	0.98	0.97	0.95	0.80
	1.1	0.99	0.99	0.99	0.98	0.98	0.98	0.98	0.98	0.98	0.97	0.95	0.93	
	1.3	0.98	0.98	0.98	0.97	0.98	0.97	0.97	0.97	0.96	0.95	0.94	0.90	
	1.5	0.97	0.97	0.97	0.97	0.97	0.96	0.96	0.96	0.95	0.94	0.92	0.87	
	1.7	0.96	0.96	0.96	0.96	0.95	0.95	0.95	0.95	0.93	0.92	0.89	0.83	
	2	0.95	0.95	0.94	0.95	0.94	0.94	0.94	0.93	0.92	0.90	0.87	0.71	
	3	0.85	0.85	0.85	0.84	0.84	0.83	0.82	0.81	0.78	0.73	0.62		
	4	0.77	0.77	0.77	0.76	0.75	0.74	0.73	0.70	0.65	0.54			
	5	0.70	0.69	0.69	0.67	0.67	0.65	0.63	0.58	0.48				
	6	0.62	0.62	0.62	0.59	0.58	0.56	0.52	0.42					
	7	0.55	0.55	0.54	0.51	0.49	0.46	0.37						
	8	0.49	0.49	0.48	0.43	0.40	0.33							
	9	0.43	0.43	0.42	0.35	0.29								
	10	0.38	0.37	0.36	0.25									
	15	0.19	0.18	0.12										
	20	0.09	0.06											
20	*0.1*	0.98	0.97	0.97	0.98	0.98	0.98	0.98	0.98	0.99	1.00	1.00	1.00	1.00
	0.3	0.99	0.98	0.99	0.99	0.99	0.99	0.99	0.99	1.00	1.00	1.00	1.00	0.98
	0.5	0.99	0.99	0.99	1.00	1.00	1.00	1.00	1.00	1.00	1.00	1.00	0.99	0.96
	0.7	0.99	0.99	1.00	1.00	1.00	1.00	1.00	1.00	1.00	0.99	0.99	0.97	0.92
	0.9	1.00	1.00	0.99	1.00	1.00	0.99	1.00	1.00	0.99	0.99	0.98	0.96	0.82
	1.1	1.00	1.00	1.00	1.00	1.00	0.99	0.99	0.99	0.99	0.98	0.96	0.94	
	1.3	1.00	1.00	1.00	0.99	0.99	0.98	0.99	0.99	0.97	0.97	0.94	0.91	
	1.5	1.00	0.99	0.99	0.99	0.99	0.98	0.98	0.97	0.97	0.95	0.93	0.88	
	1.7	0.99	0.99	0.98	0.98	0.98	0.97	0.97	0.96	0.95	0.94	0.91	0.84	
	2	0.98	0.98	0.98	0.98	0.97	0.96	0.96	0.95	0.94	0.92	0.88	0.72	
	3	0.92	0.92	0.92	0.90	0.89	0.88	0.87	0.85	0.81	0.76	0.65		
	4	0.86	0.86	0.86	0.84	0.82	0.80	0.78	0.75	0.69	0.59			
	5	0.80	0.80	0.79	0.76	0.74	0.71	0.68	0.62	0.53				
	6	0.74	0.73	0.72	0.68	0.65	0.62	0.56	0.46					
	7	0.67	0.67	0.66	0.60	0.56	0.51	0.42						

(Continued)

Table A1. (Continued)

(c)

field size diameter [cm]	depth [cm]	thickness of backscatter material [cm]												
		30	20	15	10	9	8	7	6	5	4	3	2	1
	8	0.61	0.60	0.59	0.51	0.46	0.38							
	9	0.55	0.54	0.53	0.41	0.33								
	10	0.49	0.49	0.47	0.30									
	15	0.28	0.26	0.16										
	20	0.15	0.09											
30	*0.1*	0.96	0.96	0.96	0.97	0.97	0.98	0.99	0.99	0.99	0.99	0.99	1.00	1.00
	0.3	0.98	0.98	0.98	0.98	0.98	0.98	0.99	1.00	1.00	1.00	1.00	1.00	0.98
	0.5	0.99	0.99	0.99	0.99	0.99	1.00	1.00	1.00	1.00	1.00	1.00	0.99	0.97
	0.7	0.99	0.99	0.99	1.00	1.00	1.00	1.00	1.00	0.99	0.99	0.99	0.98	0.93
	0.9	0.99	0.99	0.99	1.00	1.00	1.00	1.00	1.00	0.99	0.99	0.98	0.96	0.82
	1.1	1.00	1.00	1.00	1.00	1.00	0.99	0.99	0.99	0.99	0.98	0.96	0.94	
	1.3	1.00	1.00	1.00	1.00	1.00	0.99	0.99	0.99	0.98	0.96	0.95	0.91	
	1.5	1.00	1.00	0.99	0.99	0.99	0.99	0.99	0.98	0.97	0.96	0.92	0.88	
	1.7	1.00	1.00	0.99	0.98	0.98	0.98	0.98	0.97	0.95	0.94	0.91	0.84	
	2	1.00	0.99	0.99	0.98	0.97	0.97	0.97	0.96	0.94	0.92	0.88	0.70	
	3	0.95	0.94	0.94	0.92	0.91	0.89	0.88	0.86	0.82	0.76	0.64		
	4	0.90	0.90	0.89	0.85	0.84	0.82	0.80	0.76	0.69	0.58			
	5	0.85	0.84	0.83	0.79	0.76	0.74	0.70	0.64	0.54				
	6	0.79	0.78	0.77	0.70	0.68	0.64	0.58	0.48					
	7	0.73	0.72	0.71	0.63	0.59	0.53	0.46						
	8	0.67	0.66	0.64	0.54	0.48	0.40							
	9	0.62	0.61	0.58	0.45	0.36								
	10	0.56	0.55	0.51	0.37									
	15	0.34	0.31	0.19										
	20	0.19	0.12											

(d)

field size diameter [cm]	depth [cm]	thickness of backscatter material [cm]												
		30	20	15	10	9	8	7	6	5	4	3	2	1
	0.1	1.00	1.00	1.00	1.00	1.00	1.00	1.00	1.00	1.00	1.00	1.00	1.00	0.99
	0.3	0.98	0.98	0.98	0.98	0.98	0.98	0.98	0.98	0.98	0.98	0.98	0.98	0.97
	0.5	0.96	0.96	0.96	0.96	0.96	0.96	0.96	0.96	0.96	0.96	0.96	0.96	0.95
	0.7	0.94	0.93	0.93	0.93	0.93	0.93	0.93	0.93	0.93	0.93	0.93	0.93	0.92
	0.9	0.91	0.91	0.91	0.91	0.91	0.91	0.91	0.91	0.91	0.91	0.91	0.91	0.79
	1.1	0.89	0.89	0.89	0.89	0.89	0.89	0.89	0.89	0.89	0.89	0.89	0.89	
	1.3	0.87	0.86	0.86	0.87	0.87	0.87	0.87	0.87	0.86	0.86	0.86	0.86	
	1.5	0.84	0.84	0.84	0.84	0.84	0.84	0.84	0.84	0.84	0.84	0.84	0.83	
	1.7	0.82	0.82	0.82	0.82	0.82	0.82	0.82	0.82	0.82	0.82	0.82	0.81	
	2	0.80	0.80	0.80	0.80	0.80	0.80	0.80	0.80	0.80	0.80	0.79	0.71	
	3	0.66	0.66	0.66	0.66	0.66	0.66	0.66	0.66	0.65	0.65	0.53		
	4	0.57	0.57	0.57	0.57	0.57	0.57	0.57	0.57	0.56	0.45			
	5	0.49	0.49	0.49	0.49	0.49	0.49	0.49	0.49	0.40				
	6	0.43	0.43	0.43	0.43	0.43	0.43	0.42	0.35					
	7	0.37	0.37	0.37	0.37	0.37	0.37	0.28						
	8	0.32	0.32	0.32	0.32	0.32	0.23							
	9	0.28	0.28	0.28	0.28	0.20								
	10	0.24	0.24	0.24	0.18									
	15	0.12	0.12	0.07										
	20	0.06	0.03											
5	*0.1*	1.00	1.00	1.00	1.00	1.00	1.00	1.00	1.00	1.00	1.00	1.00	1.00	1.00
	0.3	1.00	1.00	1.00	1.00	1.00	1.00	1.00	1.00	1.00	1.00	0.99	0.99	0.99
	0.5	0.99	0.99	0.99	0.99	0.99	0.99	0.99	0.99	0.99	0.99	0.99	0.98	0.97
	0.7	0.98	0.98	0.98	0.98	0.98	0.98	0.98	0.98	0.98	0.98	0.97	0.97	0.94
	0.9	0.97	0.97	0.97	0.97	0.97	0.97	0.97	0.97	0.97	0.97	0.96	0.95	0.77
	1.1	0.96	0.96	0.96	0.96	0.96	0.96	0.96	0.96	0.95	0.95	0.95	0.93	
	1.3	0.95	0.94	0.95	0.94	0.94	0.94	0.94	0.94	0.94	0.94	0.93	0.91	
	1.5	0.93	0.93	0.93	0.93	0.93	0.93	0.93	0.93	0.92	0.92	0.91	0.88	

(Continued)

Table A1. (Continued)

(d)

field size diameter [cm]	depth [cm]	thickness of backscatter material [cm]												
		30	20	15	10	9	8	7	6	5	4	3	2	1
	1.7	0.92	0.92	0.92	0.91	0.92	0.91	0.91	0.91	0.91	0.90	0.89	0.85	
	2	0.90	0.90	0.90	0.90	0.90	0.90	0.90	0.89	0.89	0.88	0.87	0.70	
	3	0.78	0.78	0.78	0.78	0.78	0.78	0.77	0.77	0.76	0.73	0.59		
	4	0.70	0.70	0.70	0.69	0.69	0.69	0.68	0.67	0.65	0.52			
	5	0.62	0.62	0.62	0.61	0.61	0.61	0.60	0.58	0.46				
	6	0.55	0.55	0.54	0.54	0.53	0.53	0.51	0.40					
	7	0.48	0.48	0.48	0.47	0.46	0.45	0.35						
	8	0.42	0.42	0.42	0.40	0.39	0.31							
	9	0.37	0.37	0.37	0.34	0.27								
	10	0.32	0.32	0.32	0.24									
	15	0.17	0.16	0.12										
	20	0.08	0.06											
10	*0.1*	1.00	1.00	0.99	1.00	1.00	1.00	1.00	1.00	1.00	1.00	1.00	1.00	1.00
	0.3	1.00	1.00	1.00	1.00	1.00	1.00	1.00	1.00	1.00	1.00	1.00	0.99	0.99
	0.5	1.00	1.00	1.00	1.00	1.00	1.00	1.00	1.00	1.00	1.00	0.99	0.99	0.97
	0.7	1.00	1.00	1.00	0.99	0.99	0.99	0.99	0.99	0.99	0.99	0.98	0.97	0.94
	0.9	0.99	0.99	0.99	0.99	0.99	0.99	0.99	0.99	0.98	0.98	0.97	0.96	0.82
	1.1	0.99	0.98	0.98	0.98	0.98	0.98	0.98	0.98	0.98	0.97	0.96	0.94	
	1.3	0.98	0.98	0.97	0.97	0.97	0.97	0.97	0.97	0.96	0.96	0.95	0.92	
	1.5	0.97	0.97	0.97	0.97	0.97	0.96	0.96	0.96	0.95	0.94	0.93	0.90	
	1.7	0.96	0.96	0.96	0.96	0.95	0.95	0.95	0.95	0.94	0.93	0.91	0.87	
	2	0.95	0.95	0.95	0.94	0.94	0.94	0.94	0.93	0.92	0.91	0.89	0.75	
	3	0.86	0.86	0.86	0.85	0.85	0.84	0.84	0.83	0.81	0.77	0.65		
	4	0.79	0.79	0.79	0.78	0.77	0.77	0.75	0.74	0.70	0.59			
	5	0.72	0.72	0.71	0.70	0.69	0.68	0.67	0.63	0.53				
	6	0.65	0.65	0.65	0.63	0.62	0.60	0.57	0.47					
	7	0.59	0.58	0.58	0.55	0.54	0.51	0.42						
	8	0.52	0.52	0.52	0.48	0.45	0.37							
	9	0.47	0.46	0.46	0.40	0.34								
	10	0.42	0.41	0.40	0.29									
	15	0.23	0.22	0.16										
	20	0.12	0.08											
20	*0.1*	0.98	0.98	0.98	0.99	0.99	0.99	0.98	0.99	0.99	1.00	1.00	1.00	1.00
	0.3	0.99	0.99	0.99	0.99	1.00	1.00	1.00	1.00	1.00	1.00	1.00	1.00	0.99
	0.5	1.00	1.00	1.00	1.00	0.99	1.00	0.99	1.00	1.00	1.00	1.00	0.99	0.97
	0.7	1.00	1.00	1.00	1.00	1.00	1.00	1.00	0.99	0.99	1.00	0.99	0.98	0.95
	0.9	0.99	1.00	1.00	1.00	0.99	1.00	0.99	0.99	0.99	0.99	0.98	0.96	0.85
	1.1	1.00	1.00	1.00	1.00	0.99	0.99	0.99	0.99	0.99	0.98	0.96	0.95	
	1.3	1.00	0.99	1.00	0.99	0.99	0.99	0.98	0.98	0.97	0.97	0.95	0.93	
	1.5	0.99	0.99	0.99	0.98	0.98	0.98	0.97	0.97	0.97	0.96	0.94	0.90	
	1.7	0.99	0.99	0.99	0.98	0.98	0.97	0.97	0.96	0.95	0.94	0.92	0.87	
	2	0.98	0.98	0.98	0.98	0.96	0.97	0.96	0.95	0.94	0.93	0.90	0.76	
	3	0.92	0.92	0.92	0.90	0.90	0.89	0.88	0.86	0.83	0.79	0.68		
	4	0.87	0.87	0.86	0.85	0.83	0.82	0.80	0.77	0.73	0.63			
	5	0.81	0.81	0.81	0.78	0.76	0.74	0.71	0.67	0.57				
	6	0.75	0.75	0.75	0.70	0.68	0.66	0.61	0.51					
	7	0.70	0.70	0.68	0.63	0.60	0.56	0.47						
	8	0.64	0.64	0.62	0.55	0.51	0.42							
	9	0.59	0.58	0.56	0.47	0.39								
	10	0.53	0.53	0.50	0.35									
	15	0.32	0.30	0.22										
	20	0.18	0.13											
30	*0.1*	0.97	0.98	0.97	0.98	0.98	0.98	0.99	0.99	0.99	1.00	1.00	1.00	1.00
	0.3	0.98	0.99	0.99	0.99	0.99	0.99	0.99	1.00	1.00	1.00	1.00	1.00	0.99
	0.5	0.99	0.99	0.99	0.99	0.99	0.99	0.99	1.00	1.00	1.00	1.00	0.99	0.97
	0.7	0.99	1.00	0.99	1.00	1.00	1.00	1.00	1.00	1.00	0.99	0.99	0.98	0.94

(Continued)

Table A1. (Continued)

(d)

field size diameter [cm]	depth [cm]	thickness of backscatter material [cm]												
		30	20	15	10	9	8	7	6	5	4	3	2	1
	0.9	0.99	1.00	1.00	1.00	1.00	1.00	1.00	0.99	0.99	0.99	0.98	0.96	0.83
	1.1	1.00	1.00	1.00	0.99	0.99	0.99	0.99	0.98	0.98	0.99	0.97	0.95	
	1.3	1.00	1.00	1.00	0.99	0.99	0.99	0.99	0.98	0.98	0.97	0.95	0.93	
	1.5	1.00	1.00	0.99	0.99	0.99	0.98	0.98	0.98	0.97	0.96	0.94	0.90	
	1.7	0.99	1.00	0.99	0.98	0.98	0.98	0.98	0.97	0.95	0.95	0.92	0.87	
	2	0.99	0.98	0.99	0.98	0.97	0.97	0.97	0.96	0.94	0.94	0.90	0.78	
	3	0.94	0.95	0.94	0.92	0.91	0.90	0.89	0.87	0.84	0.80	0.70		
	4	0.90	0.90	0.89	0.86	0.85	0.83	0.82	0.79	0.73	0.64			
	5	0.86	0.86	0.84	0.80	0.78	0.76	0.73	0.68	0.59				
	6	0.80	0.80	0.79	0.73	0.71	0.68	0.63	0.53					
	7	0.75	0.75	0.73	0.66	0.63	0.58	0.51						
	8	0.70	0.70	0.67	0.58	0.53	0.45							
	9	0.65	0.65	0.61	0.49	0.40								
	10	0.60	0.59	0.55	0.38									
	15	0.38	0.36	0.23										
	20	0.23	0.15											

ORCID iDs

Anna Subiel https://orcid.org/0000-0002-3467-4631
Ileana Silvestre Patallo https://orcid.org/0000-0003-0467-3870
Hugo Palmans https://orcid.org/0000-0002-0235-5118
Georgios Soultanidis https://orcid.org/0000-0001-9620-1728
John Greenman https://orcid.org/0000-0002-6003-6051
Christopher Cawthorne https://orcid.org/0000-0002-5975-0354

References

Aird EGA, Radiology BIo, Physics Io, Medicine Ei and Biology 1996 Central axis depth dose data for use in radiotherapy *A Survey of This Supplement Depth Doses and Related Data Measured in Water or Equivalent Media* (London: British Institute of Radiology) (https://www.worldcat.org/title/central-axis-depth-dose-data-for-use-in-radiotherapy-1996-a-survey-of-depth-doses-and-related-data-measured-in-water-or-equivalent-media/oclc/036632731)

Andreo P 2019 Data for the dosimetry of low- and medium-energy kV x rays *Phys. Med. Biol.* **64** 205019

Andreo P, Burns D T and Hohlfeld K 2004 Absorbed dose determination in external beam radiotherapy: an international code of practice for dosimetry based standards of absorbed dose to water *IAEA TRS-398* 66–81

Aukett R J, Burns J E, Greener A G, Harrison R M, Moretti C, Nahum A E and Rosser K E 2005 Addendum to the IPEMB code of practice for the determination of absorbed dose for x-rays below 300 kV generating potential (0.035 mm Al–4 mm Cu HVL) *Phys. Med. Biol.* **50** 2739–48

Bass G A D S, Kelly M, Manning J W, Maughan D J, Nutbrown R F, Sander T and Shipley D R 2019 The NPL Air Kerma Primary Standard Free-Air Chamber For Medium Energy X-Rays: summary Of Factors Incorporating ICRU Report 90 Recommendations *NPL Report IR 54*, Teddington

Berger M J and Hubbell J H 1987 XCOM: photon Cross Sections on a Personal Computer *NIST Report*, Gaithersburg, MD

Brahme A 1984 Dosimetric Precision Requirements in Radiation Therapy *Acta Radiol. Oncol.* **23** 379–91

British Institute of R, Institute of P, Engineering in M and Biology 1996 Central axis depth dose data for use in radiotherapy *A Survey of Depth Doses and Related Data Measured in Water or Equivalent Media* (British Journal of Radiology Supplement No. 25) (London: British Institute of Radiology)

Chen Q, Molloy J, Izumi T and Sterpin E 2019 Impact of backscatter material thickness on the depth dose of orthovoltage irradiators for radiobiology research *Phys. Med. Biol.* **64**

Chica U, Anguiano M and Lallena A M 2008 Study of the formalism used to determine the absorbed dose for low-energy x-ray beams *Phys. Med. Biol.* **53** 6963–77

Desrosiers M, DeWerd L, Deye J, Lindsay P, Murphy M K, Mitch M, Macchiarini F, Stojadinovic S and Stone H 2013 The importance of dosimetry standardization in radiobiology *J. Res. Natl Inst. Stand. Technol.* **118**

Dos Santos M, Paget V, Ben Kacem M, Trompier F, Benadjaoud M A, Francois A, Guipaud O, Benderitter M and Milliat F 2018 Importance of dosimetry protocol for cell irradiation on a low X-rays facility and consequences for the biological response *Int. J. Radiat. Biol.* **94** 597–606

Draeger E, Sawant A, Johnstone C, Koger B, Becker S, Vujaskovic Z, Jackson I-L and Poirier Y 2020 A Dose of reality: how 20 years of incomplete physics and dosimetry reporting in radiobiology studies may have contributed to the reproducibility crisis *Int. J. Radiat. Oncol. Biol. Phys.* **106** 243–52

Grosswendt B 1990 Dependence of the photon backscatter factor for water on source-to-phantom distance and irradiation field size *Phys. Med. Biol.* **35** 1233–45

Grosswendt B 1993 Dependence of the photon backscatter factor for water on irradiation field size and source-to-phantom distances between 1.5 and 10 cm *Phys. Med. Biol.* **38** 305–10

Guterman L 2015 Irreproducible life sciences research in the U.S. costs $28 billion (https://www.sciencenews.org/article/irreproducible-life-sciences-research-us-costs-28-billion)

Harrison R M 1982 Backscatter factors for diagnostic radiology (1-4 mm Al HVL) *Phys. Med. Biol.* **27** 1465–74

Hubbell J H and Seltzer S M 2004 *Tables of X-ray Mass Attenuation Coefficients and Mass-Energy Absorption Coefficients* NIST Standard Reference Database 126 (Gaithersburg, MD: NIST) (https://doi.org/10.18434/T4D01F)

ICRU 1976 Determination of absorbed dose in a patient irradiated by beams of X or gamma rays in radiotherapy *ICRU Report 24*, Bethesa, MD

InnovateUK 2018 Development of a multipurpose small animal phantom for pre-clinical radiotherapy studies 2015–2018 *InnovateUK project* (Ref N. 102524) (https://www.npl.co.uk/projects/pre-clinical-dosimetry-service)

Kawrakow I, Rogers D W O, Tessier F and Walters B R B 2018 The EGSnrc Code System: Monte Carlo Simulation of Electron and Photon Transport *NRCC Report* (Ottawa, Canada: NRCC)

Kegel P, Riballo E, Kuhne M, Jeggo P A and Lobrich M 2007 X-irradiation of cells on glass slides has a dose doubling impact *DNA Repair (Amst.)* **6** 1692–7

Kim J, Hill R, Mackonis E C and Kuncic Z 2010 An investigation of backscatter factors for kilovoltage x-rays: a comparison between Monte Carlo simulations and Gafchromic EBT film measurements *Phys. Med. Biol.* **55** 783–97

Klevenhagen S C 1982 The build-up of backscatter in the energy range 1 mm Al to 8 mm Al HVT *Phys. Med.Biol.* **27** 1035

Klevenhagen S C, Aukett R J, Harrison R M, Moretti C, Nahum A E and Rosser K E 1996 The IPEMB code of practice for the determination of absorbed dose for x-rays below 300 kV generating potential (0.035 mm Al-4 mm Cu HVL; 10-300 kV generating potential) *Phys. Med. Biol.* **41** 2605–25

Knight R T and Nahum A E 1994 *Dept and Field Size Dependence of Ratios of Mass Energy Absorption Coefficient, Water to Air, for Kilovoltage X Ray Dosimetry* (Vienna: International Atomic Energy Agency (IAEA))

Lu L C, Bondra K, Gupta N, Sommerfeld J, Chronowski C, Leasure J, Singh M and Pelloski C E 2013 Using NanoDot dosimetry to study the RS 2000 X-ray Biological Irradiator *Int. J. Radiat. Biol.* **89** 1094–9

Ma C M, Coffey C W, DeWerd L A, Liu C, Nath R, Seltzer S M and Seuntjens J P 2001 AAPM protocol for 40-300 kV x-ray beam dosimetry in radiotherapy and radiobiology *Med. Phys.* **28** 868–93

Mayles P E, Nahum A E and Rosenwald J E 2007 *Handbook of Radiotherapy Physics* (Boca Raton, FL: CRC Press)

Nature 2018 Design preclinical studies for reproducibility 2018 *Nat. Biomed. Eng.* 2 789–90
Poludniowski G and Evans P 2007 Calculation of x-ray spectra emerging from an x-ray tube. Part I. Electron penetration characteristics in x-ray targets *Med. Phys.* **34** 2164–74
Poludniowski G G 2007 Calculation of x-ray spectra emerging from an x-ray tube. Part II. X-ray production and filtration in x-ray targets *Med. Phys.* **34** 2175–86
Rogers D W O, Kawrakow I, Seuntjens J, Walters B R B and Mainegra-Hing E 2018 NRC User Codes for EGSnrc *NRCC Report*, Ottawa, Canada
Subiel A, Ashmore R and Schettino G 2016 Standards and methodologies for characterizing radiobiological impact of high-z nanoparticles *Theranostics* **6** 1651–71
Verhaegen F *et al* 2018 ESTRO ACROP: technology for precision small animal radiotherapy research: optimal use and challenges *Radiother. Oncol.* **126** 471–8
Yoshizumi T, Brady S L, Robbins M E and Bourland J D 2011 Specific issues in small animal dosimetry and irradiator calibration *Int. J. Radiat. Biol.* **87** 1001–10
Zoetelief J, Broerse J J, Davies R W, Octave-Prignot M, Rezvani M, Vergara J C S and Toni M P 2001 Protocol for X-ray dosimetry in radiobiology *Int. J. Radiat. Biol.* **77** 817–35
Zoetelief J, Davies R W, Scarpa G, Hofmeester G H, Dixon-Brown A, van der Kogel A J and Broerse J J 1985 Protocol for x-ray dosimetry and exposure arrangements employed in studies of late somatic effects in mammals *Int. J. Radiat. Biol.* **47** 81–102